RESISTANCE PREDICTION METHOD FOR SEMI-PLANING CATAMARANS WITH SYMMETRICAL DEMIHULLS

report
"afstudeer opdracht"
Maritieme Techniek
TH Delft

by: A.J. Oving
Wageningen, December 1985

CONTENTS: Page:

CONTENTS (continued):

LIST OF SYMBOLS

AR	- aspect ratio: B/L_{WL}
A_T	- immersed transom area
A_x	- midship section area
B	- beam of demihull at load waterline
Cb	- blockcoefficient
Cp	- prismatic coefficient
Fn	- Froudenumber $(V/\sqrt{g.L})$
F_{nT}	- depth Froudenumber $(V/\sqrt{g.T})$
$F_{n.\nabla}$	- volume Froudenumber $(V/\sqrt{g.\nabla^{1/3}})$
G	- Green's function
g	- acceleration due to gravity
IF_{wp}	- wave interference factor ($\simeq$ RWI/RW)
L	- length
L_{HD}	- hydrodynamic lift
L_{WL}	- length on load waterline
R_{FR}	- skin friction resistance
R_{HS}	- hydrostatic resistance (due to transom)
R_T	- total resistance (bare hull)
R_W	- wave resistance (without interference resistance)
R_{WI}	- wave interference resistance
S	- hullspacing; distance between the centreplanes
S_W	- wetted surface (transom area excluded)
T	- draught
t(x,y)	- local half beam of demihull
U	- free stream velocity or speed of catamaran
XG	- position of the centre of gravity aft of the fore perpendicular
β	- deadrise angle
Δ	- displacement
Φ	- velocity potential
ϕ	- perturbation velocity potential
λ	- wave length
μ	- doublet density

ρ - density of water
σ - source density
τ - trim angle
$\zeta(x,z)$ - waveheight

ABSTRACT

A resistance prediction method (program CATRES) has been developed for semi-planing catamarans with symmetrical demihulls.
Total resistance is determined by summation of four resistance components:

1. twice the waveresistance of a demihull in isolation
2. twice the waveinterference resistance of one demihull
3. hydrostatic resistance due to separation of the flow at the transom (ventilation)
4. skin friction resistance

Thin ship theory is used for the determination of the wave- and waveinterference resistance. As a consequence of the thin ship approach, the effects of wave reflection and of bodyinterference upon the waveinterference resistance are neglected. Concerning the transom the open stern model is adopted.
The hydrostatic resistance follows from integration of hydrostatic pressures over the ventilated part of the transom. Skin friction resistance is related to the wetted surface and an analytically derived form factor.

The method is applied to five testcases. For hullspacings larger than a quarter of the demihull length and Froudenumbers not in excess of 1.0, correlation with model testresults is good. The prediction of sinkage, trim and the hydrostatic resistance is only moderate. Poor prediction of the hydrostatic resistance was found at Froude numbers in excess of .7.

Most important conclusion is that the method recognises main differences (> 10%) between the resistance characteristics of different designs.

INTRODUCTION

The hydrodynamic aspects of high speed catamarans have been studied very little. Up to now most investigations were centered on displacement type catamarans. Recently, however, a steady growth of the interest in the hydrodynamic aspects of high speed catamarans took place, which is mainly due to the steady increase of commercial applications. In spite of these developments there is still a lack of resistance prediction methods for these catamarans. Therefore a study was initiated, with as its principle goal, the development of a resistance prediction method for semi-planing catamarans. A previous report [22] comprises the first two steps of this study; i.e. study of the resistance and resistance components and an evaluation of several approaches to the catamaran resistance prediction problem. On the basis of this preliminary study it was decided to restrict oneself to catamarans with symmetrical component hulls and to take the thin ship theory as starting point for the resistance prediction method.

This report deals with the final prediction method (program CATRES). Chapter 1 gives general background information, the subject is further specified and a brief summary of recent resistance prediction methods is given. Chapter 2 deals with the resistance prediction method as such. It comprises a discussion of the resistance model, followed by a description of the numerical evaluation of the resistance components. The program CATRES has been applied to several testcases. The results are presented and discussed in Chapter 3. Final remarks and main conclusions are presented in Chapter 4.

1. GENERAL

As semi-planing catamarans and the related resistance problems have been little studied in the past, they need some specification.

In the first Section, the term semi-planing catamarans is defined and specified. Section 1.2 deals with the complex resistance characteristics and comprises an outline of the flow phenomena and mechanisms most relevant to the subject. In the final Section a brief discussion of current resistance prediction methods is given.

1.1. Concept definitions

First two definitions need to be given:

- semi-planing catamarans: catamarans which rely partially upon hydrodynamic load relief, while, throughout the speedrange, the buoyant forces are predominant for the vertical equilibrium,
- demihull: the component hull of a catamaran.

For convenience, semi-planing catamarans made up from symmetrical demihulls are simply denoted by "catamarans".

Applications to which the catamaran lends itself are as a passenger ferry, supply/crew boat, police/rescue boat etc.. For all these missions payload is a small fraction of displacement and a high priority is put on maintenance of a schedule regardless of weather conditions. The catamaran, however, is not the only vessel which lends itself to these missions. Planing boats, hydrofoil craft, hovercrafts and surface effect ships may also be considered. Figure 1 gives a first impression of the competitive position of caramarans relative to other high speed craft. Comparison of the transport efficiency, however, is not conclusive as every design study should include consideration of the operation conditions, the restrictions and the economics of a certain design.

Nevertheless, some kind of evaluation of the merits of the

catamaran concept is possible by considering its main advantages and disadvantages: [12] [20]:[1)]

advantages: - the exceptionally high transverse stability
- the large deck area
- compared to monohulls, less restrictions are imposed upon the hullform, resulting in more flexibility in hull form design

disadvantage: - the large wetted area coefficient: $S_w/\nabla^{2/3}$. (2)

Concerning the resistance Michell [20] and Fry & Graul [12] pointed out that catamarans may have favourable resistance characteristics at high displacement and semi-planing speeds. Both at low speeds, as well as at planing speeds, catamarans feature poor performance. At low speeds this is due to the predominance of the frictional resistance in combination with the relatively large wetted area. At planing speeds the poor performance results from the small values of the aspect ratio (B/L_{WL}). For a constant wetted planing area the hydrodynamic resistance increases with decreasing aspect ratio. This is similar in concept to the increased drag of a biplane wing over a monoplane of the same area but twice the span. The superior resistance characteristics in the favourable speed-range are partially due to the fact that the typical humpdrag is less pronounced (see Fig. 2). This results from the small trim angles associated with long and slender hulls.

---

1) number between brackets correspond to number in list of references

2) symbols as defined in the list of symbols

Two recent catamaran designs are shown in Figure 3. In general, the hullforms feature a fine bow form, almost parallel sides along the run and a cut-off transom stern for a clean separation of the flow. Predominant are hard chine hulls with deep vee sections near the stem merging into flat vee sections near the stern. The propulsion is either by means of conventional propellers mounted on an inclined shaft or by means of waterjet propulsion (draft restrictions). Conventional propeller propulsion goes together with typical planing hull appendages.

Some typical values for recent catamaran designs are:

$\Delta \quad \leq$ 100 tonnes

$L \quad \leq$ 40 m

$Fn \quad \leq 1.2$

$L_{HD}/\Delta \leq 0.4$ (approximately at Fn = 1.2)

$0.20 \leq S/L_{WL} \leq 0.4$

$13 \leq L_{WL/T} \leq 25$

$8 \leq L_{WL/B} \leq 10$

where: L_{HD} = hydrodynamic lift

S = centreline based hullspacing (W-B)

1.2 Interference effects

The catamaran resistance problem is a complex matter, which is mainly due to complicated interference effects between the demihulls. For a better understanding of the resistance problem and the related mechanisms these interference effects are briefly discussed in the following. For a more comprehensive discussion of the catamaran resistance problem reference is made to [22]

Two types of interference can be discerned:

- waveinterference, which is due to the superposition of two wavesystems, each associated with a demihull in isolation,
- body interference, which is the change of flow about one demihull due to the presence of the other demihull.

Wave interference

Wave interference determines to a large extent the final wavepattern around a catamaran and is due to the superposition of the two wavesystems, each created by one demihull.
The two wavesystems may reinforce eachother and thus create a large wavemaking resistance. They may also partially cancel eachother and greatly reduce wavemaking. Everest [10] showed from a wavepattern analysis that beneficial wave interference is achieved by the cancellation of part of the component hulls divergent wavesystem, while adverse interference effects arise on interaction of the more transverse waves. This is due to the fact that the phase differences between the transverse waves are, in general, smaller than the phase differences between the divergent waves.

The wave interference effects may be expressed quantitatively by means of the wave interference factor (IF_{wp}):

$$IF_{wp} = \Delta R_{wp}/2DR_{wp}$$

where:

ΔR_{wp} - wavepattern resistance of catamaran minus twice the wavepattern resistance of the demihull in isolation

DR_{wp} - wavepattern resistance of demihull in isolation.

First order wave resistance formulations (Eggers [8], Tasaki [29]) show that the wave interference factor can be divided into two parts:

- a monotonic and positive term which is a monotonically decreasing function with respect to the increase of the product: $(S/L_{WL})*(1/Fn^2)$.
- a term which oscillates from plus to minus. This term oscillates with respect to the Froudenumber and does not change rapidly with respect to the distance between the demihulls.

Figs. 4 and 5 depict the relationships between the interference factor, the Froude number and the hullspacing, as found by Tasaki for a mathematical hullform. In general, experiments (e.g. Everest [10]) confirm this behaviour, however, they show slightly smaller beneficial and adverse interference effects.

Figure 5 shows that beneficial wave interference effects are restricted to the pre-hump speed range (Fn ≈ 0.4). Maximum values are centered around: $S/L_{WL} \approx 0.3$ and Fn ≈ 0.3. For the catamarans considered, the adverse interference effects are most important because their maximum value is reached in the hump speed range (Fn=0.4-0.5). In this speed range most of the wave energy is related to the more transverse waves. As the wave energy is more and more concentrated in the divergent waves, adverse interference effects slowly decrease when speed increases from Fn=0.5. Beside the parameters: Fn and S/L_{WL}, the ratio of transom area to main section area also affects the wave interference.
The maximum value for the adverse wave interference effects decreases with increasing A_T-Ax ratio because the stern wavesystem becomes less pronounced.

Body interference

Body interference is characterised by complex inter-relations. Consider a hull with port and starboard symmetry moving abreast an identical hull. Then the flow around a demihull is no longer symmetric and may be divided in a symmetrical and an asymmetrical part. It is noted that the flow is equivalent to the flow around a demihull moving along a rigid wall at a distance of half the hullspacing.

Speaking in terms of velocities, the symmetrical part is composed of three components: the free stream velocity, the perturbation velocity due to the demihull, and the perturbation velocity generated by the other demihull.

The asymmetric part of the flow is due to the operation of the demihull in the curved flow field created by the other demihull (Figure 6). This is similar to a cambered hull towed in a uniform flow at an angle of attack. A circulating flow around the demihull exists resulting in a crossflow over the keel, which can influence the eddying resistance (Pien [23]). Vortex shedding results from the lift generation together with the finite aspect ratio (T/L_{WL}) of the demihulls. The vortices give rise to induced drag which may be large at low hull spacings.

1.3 Resistance prediction methods

During the years several prediction methods for the resistance of catamarans have been developed. These methods fall apart in two groups:

- wave resistance prediction methods for catamarans operating in the displacement mode
- resistance prediction methods for planing mode conditions.

Wave resistance prediction methods

Thin ship formulations of the catamaran wave resistance problem have been set up by Eggers [8] and Lunde [18]. Eggers came up with a Michell-Sretensky formulation and obtained closed form solutions for mathematical hullforms. Lunde, on the other hand, formulated the problem along the lines of Havelock's theory.
More recently several thin ship programs have been developed for the similar case of Small Waterplane Area Twin Hull (SWATH) ships (Kusaka [15], Lin [17], Chapman [5]. These three programs only take thickness effects into account and impose severe restrictions upon the hull- (strut-) form. The programs from Lin and Chapman are available at NSMB and have been extensively studied by Allema [1]. Allema's study shows a good predictive capability of these two programs for Froude numbers not exceeding 0.7.

Pien [23], took another approach. He represented the hull by a doublet distribution on and normal to the hull surface below its waterline and a line source and line doublet distribution along the load waterline. Densities of these distributions are determined by solving the inner flow problem: i.e. the condition of having U.x as the velocity potential within the displacement volume of the ship. Good correlation is found between predicted and measured residuary resistance coefficients for SWATH ships.

Everest's wavepattern resistance prediction method [10] is based upon the wavepattern analysis method from Eggers [9]. The wave pattern resistance is derived from wave pattern data which are obtained by the linear superposition of the wave patterns of the demihulls. The wavepatterns of the demihulls may be determined either theoretically or by means of experimental techniques. As a consequence of this approach he neglects the effects of wave-reflection and body interference. The method has been applied to semi-planing catamarans, however, Everest did not compare the results with results from experiments [11].

Tanaka et al. [28] applied the Hess & Smith panel method [14] to both symmetrical as well as asymmetrical catamarans. The hull is represented by panels laid over the hull surface, each of them having a constant, rankine source density. Agreement between the calculated and measured pressure distribution over the sections is poor. This is presumably due to the fact that the free surface effect is neglected.

Prediction methods for planing catamarans

Two performance prediction methods for planing catamarans have been developed. Both are based on the assumption that the interference effects are negligible. The catamaran resistance is taken as twice the demihull resistance.

Clement [6] developed a graphical method for the prediction of the "ideal high-speed resistance" of planing catamarans.
Application is restricted to:

- low aspect ratio hulls: $0.1 \leq AR \leq 0.3$
- small deadrise angles: $0 \leq \beta \leq 10°$
- high planing speeds where hydrodynamic lift is predominant.

The method is rather cumbersome when the resistance has to be predicted for a given speed. No resistance predictions could be obtained for relatively low speeds ($F_n \leq 1.0$). Furthermore, the method seems to give unreliable results. Application of Clements method to the catamaran "Shuman" ([12]) resulted in a predicted $^{RT}/_{\Delta}$ value at 40 knots which is lower than the measured $^{RT}/_{\Delta}$ value at 18 knots. As the mean deadrise angle was 22°, the $^{RT}/_{\Delta}$ value was obtained by extrapolation. Nevertheless, doubt arises as to the accuracy of Clements method.

Sherman and Fisher [27] presented a listing of a performance prediction method for planing catamarans. It is a modification of Savitsky's planing performance prediction method [25].
Consequently it is restricted in application to prismatic hullforms with:

- a clean separation of the flow at the transom and chines
- a non immersed bow

Furthermore, the empirical formulas for lift, wetted surface and centre of pressure are restricted in application to:

$$2° \leq \tau \leq 15°$$
$$10° \leq \beta \leq 30°$$
$$\lambda \leq 4$$

where:

τ = trim angle
β = deadrise angle
λ = mean wetted length to beam ratio

2. RESISTANCE CALCULATION

Consider the basic requirements which should be met by a resistance prediction method for semi-planing catamarans.
The method should be:

- capable to deal with current symmetrical demihull forms which feature a transom stern
- applicable at speeds corresponding to Froudenumbers not exceeding a value of 1.0-1.2
- capable to estimate the wave interference resistance

None of the methods discussed in the foregoing can meet the above requirements. The methods designed for SWATH ships are too specific (Kusaka, Lin, Chapman, Pien), and consequently restricted to simple hull- (strut-) forms. Everest's method is not of interest because it still requires the wavepattern to be determined. The method of Tanaka et al. suffers from a poor predictive capability.
The resistance prediction methods for planing catamarans are found to be too restricted as to hullform. Furthermore, Clement's method does not apply to semi-planing cases.

For these reasons a new resistance prediction method has been developed which is described in the following.
The resistance prediction method proceeds from the following resistance model:

$$R_T = R_W + R_{WI} + R_{HS} + R_{FR}$$

where:

- R_T - total catamaran resistance (bare hull)
- R_W - twice the wavepattern resistance of a demihull in isolation
- R_{WI} - the wave interference resistance
- R_{HS} - the hydrostatic part of the transom resistance (separation)
- R_{FR} - the skin friction resistance

The wave and wave interference resistance are evaluated according to the thin ship theory (Section 2.1). The numerical evaluation of R_{HS} and R_{FR} is discussed in Sections 2.2 and 2.3 respectively.

Section 2.4 comprises a brief discussion of the following resistance components:

R_{wb} - wavebreaking resistance
R_{ind} - induced drag
R_{spray} - spray drag

They are not incorporated in the resistance model, but may be significant in specific cases.

2.1 Wave resistance

As the wave resistance is a complex matter, a theoretical approach is taken, allowing an evaluation of the interference effects. Although current B/T-ratios plea for use of a flat ship theory, a thin ship approach has been followed. Flat ship theories have had some consideration in the past (e.g. Maruo [19], Tulin [31], Wang & Rispin [32]), however, there arise severe numerical problems as an integral equation with a very difficult kernel has to be solved. The flat ship problem can only be solved under severe restrictions to hullform and Froude number.

As the resistance is determined by the flow, the mathematical model of the flow around a catamaran is given first (Section 2.1.1). The numerical aspects of the wave resistance calculation are discussed in Section 2.1.2. The method is based on the program MICHELL [24] which calculates the wave resistance of monohulls. Therefore the emphasis is put on the evaluation of the wave interference resistance.

2.1.1 Formulation of the catamaran flow problem

A cartesian coordinate system is adopted with the x-axis directed from bow to stern (Fig. 7). The centreplanes of the demihulls (S_1, S_2) lie in the planes $z = 0$, $z = -2b$ respectively.

The total velocity potential is made up of a uniform flow term and a disturbance term caused by the hull.
Thus:

$$\Phi = U.x + \phi$$
$$\nabla\Phi = U + \nabla\phi$$

where: ϕ is the disturbance potential and $\nabla\phi = \underset{\sim}{V}$ the disturbance velocity. ($\underset{\sim}{V} = (u,v,w)$).

The exact problem

The perturbation potential must satisfy the following conditions.
- conservation of mass which requires satisfying the Laplace equation:

$$\frac{\partial^2\phi}{\partial x^2} + \frac{\partial^2\phi}{\partial y^2} + \frac{\partial^2\phi}{\partial z^2} = 0 \qquad (1)$$

  for $y \leq \zeta(x,z)$ and (x,y,z) outside the region bounded by the demihulls ($\zeta(x,z)$= waveheight).
- a kinematic boundary condition on the hull surface:

$$\frac{\partial\phi}{\partial z} = \left(U + \frac{\partial\phi}{\partial x}\right) \cdot \frac{\partial t}{\partial x} + \frac{\partial\phi}{\partial y} \cdot \frac{\partial t}{\partial y} \qquad \text{on: } z = \pm\, t(x,y)$$
$$z = -2b \pm t(x,y)$$

- from the kinematic condition at the free surface it follows that:

$$\frac{\partial\phi}{\partial z} - \left(U + \frac{\partial\phi}{\partial x}\right) \cdot \frac{\partial\zeta}{\partial x} - \frac{\partial\phi}{\partial z}\frac{\partial\zeta}{\partial z} = 0 \quad \text{on: } y = \zeta(x,z) \qquad (3)$$

- Since the pressure is constant at the free surface the disturbance potential must satisfy the following dynamic boundary condition:

$$\tfrac{1}{2}\left[\left(U + \frac{\partial\phi}{\partial x}\right)^2 + \left(\frac{\partial\phi}{\partial y}\right)^2 + \left(\frac{\partial\phi}{\partial z}\right)^2 - U^2\right] + g.y = 0 \qquad (4)$$

on: $y = \zeta(x,z)$

For an unbounded fluid the boundary conditions are completed by the radiation condition:

$$\phi = \begin{cases} O(x^2+z^2)^{-\frac{1}{2}} & , \text{ for } x \leqslant 0 \\ O(1) & , \text{ for } x \geqslant 0 \end{cases} \quad , \text{ for } x^2+y^2 \longrightarrow \infty \qquad (5)$$

The thin ship approximation

The exact problem is not easy to tackle. Therefore the thin ship assumption is adopted in order to obtain a simpler boundary value problem.

It is assumed that the ship's beam is a small parameter compared to all of the other characteristic lengths relevant to the problem. Thus B/L, B/T, $B/\lambda \ll 1$. As a consequence it may be assumed that the disturbance is small thus: u, v, $w \ll U$. Strictly speaking, the two latter assumptions (i.e. B/T, $B/\lambda \ll 1$) are incorrect in most practical cases. Nevertheless, the thin ship assumption proves to be useful.

As the beam is now a small parameter, the perturbation potential ϕ may be expanded in powers of the beam. It can be shown that the first order approximation of the perturbation potential follows from:

The Laplace equation:

$$\frac{\partial^2\phi}{\partial x^2} + \frac{\partial^2\phi}{\partial y^2} + \frac{\partial^2\phi}{\partial z^2} = 0 \qquad : \text{ for } y \leqslant 0 \qquad (7)$$

and from two linearised boundary conditions.
The free surface condition: (follows from (4))

$$\frac{\partial^2 \phi}{\partial x^2} + \frac{g}{U^2} \cdot \frac{\partial \phi}{\partial y} = 0 \qquad \text{at } y = 0 \qquad (8)$$

Thus, the condition at the free surface $y = \zeta(x,z)$ is replaced by a condition at the plane $y = 0$.

In the same way, the boundary conditions at the demihull-surfaces are replaced by conditions at their centreplanes:

$$\frac{\partial \phi}{\partial z} = \pm U \cdot \frac{\partial t}{\partial x} \qquad \text{at: } S_1,\ S_2 \qquad (9)$$
$$z = \pm 0;\ z = -2b \pm 0$$

The radiation condition (5) is not altered under the thin-ship assumption.

It is recognised that in the case of a catamaran, the flow around a symmetrical demihull is composed of a symmetric and an asymmetric term. Consequently, one may decompose the problem in a thickness and a lift problem respectively. This most fundamental approach (within the context of the thin ship theory) results in the following decomposition of the perturbation potential.

$$\phi = \phi_{1\sigma} + \phi_{2\sigma} + \phi_{1\mu} + \phi_{2\mu} \qquad (10)$$

where: $\phi_{1\sigma}$, $\phi_{2\sigma}$ - are solutions of the boundary value problem determined by (7), (8), (9): They can be associated with a source distribution over the planforms S_1, S_2.

$\phi_{1\mu}$, $\phi_{2\mu}$ - are solutions of the boundary value problem determined by (7), (8) and the following expression instead of (9).

$$\frac{\partial \phi_{1\mu}}{\partial y} + \frac{\partial \phi_{2\mu}}{\partial y} = U \cdot \frac{\partial C}{\partial x} - \frac{\partial \phi_{2\sigma}}{\partial y} \qquad (11)$$

at Sl and S2.

$\phi_{1\mu}, \phi_{2\mu}$ can be associated with a doublet

distribution over the centreplanes S1 and S2

note: C = C(x,y); the camberfunction;
C(x,y)=0 for symmetrical demihulls.

The evaluation of $\phi_{1\mu}$ and $\phi_{2\mu}$ is very difficult. Equation (11) leads to a complex integral equation, which has to be solved to obtain the doublet density distribution. Therefore, it is assumed that the asymmetric property of the flow may be neglected when dealing with symmetrical demihulls. So,

$$\phi = \phi_{1\sigma} + \phi_{2\sigma} \tag{12}$$

where: (writing ϕ_1, ϕ_2 instead of $\phi_{1\sigma}$, $\phi_{2\sigma}$)

$$\phi_1(x,y,z) = - \iint_{S_1} \sigma_1(x_o,y_o) \cdot G_1(x,y,z;x_o,y_o,0)\,dx_o dz_o \tag{13}$$

$$\phi_2(x,y,z) = - \iint_{S_2} \sigma_2(x_o,y_o) \cdot G_2(x,y,z;x_o,y_o,-2b)\,dx_o dz_o \tag{14}$$

$G_1()$ and $G_2()$ are Green's functions, which are solutions of the boundary value problem stated in the foregoing. Green's functions have the favourable property that they are independent of hull-geometry.
$\sigma_{1,2}(x_o,y_o,z_o)$ are the source density distributions. They are simply related to the hullgeometry:

$$\sigma_{1,2}(x_o,y_o) = \frac{U}{2\pi} \frac{\partial t}{\partial x} \tag{15}$$

which follows from the jump property of the derivative $\partial\phi/\partial z$ at the plane of distribution

$$\frac{\partial \phi}{\partial z}(x_o,y_o,\pm 0) = \pm 2\pi . \sigma(x_o,y_o,0)$$

The flow around a catamaran is now determined by expressions (12), (13) and (14).

Summarising, the following assumptions have been made:
- the beam is a small parameter compared to other characteristic lengths relevant to the problem. For current demihull forms, however, the draft is of the same order of magnitude as the beam.
- the flow around the demihull is symmetric. The asymmetric part is neglected. This led to hull representation by a source distribution only, thus neglecting body interference effects upon the wave resistance. Consistent with this assumption is the assumption that the induced drag may be neglected.
- the implicit assumption that the flow around a fixed model is substantially the same as the flow around a freely floating model. This assumption follows from the mathematical formulation of the thin ship problem. Consequently, the effect of hydrodynamic lift on the waveresistance is neglected. The wave resistance is calculated for a fixed model without sinkage or trim.

Furthermore it is noted that the effects of wave reflection are not accounted for by a thin ship approach. Inclusion of these effects requires an exact kinematic boundary condition on the hullsurface.

hydrodynamic modelling of the transom

The open stern model has been adopted to represent the flow phenomena around transom sterns. The flow is modelled as the flow around a semi-infinite body, composed of the ship's hull plus an infinite extension with the same shape as the transom. This model is physically correct as it allows for a rather clean separation at the transom. It results simply from a consequent application of equation 15.

2.1.2 Numerical evaluation of the waveresistance

Within CATRES a Cartesian coordinate system x,y,z is adopted, in which z = 0, z = -2b are the centreplanes of the demihulls. The x-coordinate is directed from bow (x=0) to stern, while the y-axis is vertically upward; y=0 is the undisturbed free surface (see Figure 8).
Further, all variables are non dimensionalised by the acceleration of gravity and the ship speed: U. So,

$$x = \bar{x} \cdot g/U^2 = \frac{\bar{x}}{L.F_n^2}$$

$$u = \bar{u}/U \text{ and } \phi = \bar{\phi}.g/u^3$$

where an overbar denotes the dimensional variables.

The calculation method can be classified as a panel method. A grid is laid on each planform having MM columns and NN rows. The nodal points are indicated by the indices i,j. The nodes are equidistant in x- and y-direction.
The evaluation of the wave resistance is composed of the following steps:

- determination of the source densities
- calculation of the potentials $\phi_1(i,j)$ and $\phi_2(i,j)$ at the nodal points
- calculation of the perturbation velocities in x- and y-direction.
- calculation of the wave resistance.

The nondimensional source densities (SD(i,j)) are calculated according to the non-dimensional version of expression 15:

$$\sigma(x_o,y_o,z_o) = \frac{1}{2\pi} \cdot \frac{\partial t}{\partial x}$$

where $\partial t/\partial x$ is obtained by applying three-point Lagrange

differentation in x-direction to the offsets at the nodal points: z(i,j).

For reasons of symmetry the potentials ϕ_1 and ϕ_2 need only be evaluated at one centreplane (S_1).

Consider expressions 12 and 13: (written in program nomenclature)

$$POT_1(i,j) = - \iint_{S_1} SD(ii,jj) \cdot G_1(x,y,z;x_o,y_o,o)dx_o dy_o \quad (12)$$

$$POT_2(i,j) = - \iint_{S_2} SD(ii,jj) \cdot G_2(x,y,z;x_o,y_o,-2b)dx_o dy_o \quad (13)$$

where: i,j - indicate field points
ii,jj - indicate source points

After Noblesse [21] the Green's function may be written in the following form:

$$G(\bar{x};\bar{x}_o) = -1/r + N(\bar{x}-\bar{x}'_o) + H(x-x_o).W(\bar{x}-\bar{x}'_o) \quad (16)$$

where: $r = \sqrt{((x-x_o)^2+(y-y_o)^2+(z-z_o)^2)}$

$\bar{x} = (x,y,z)$: position vector of the field point

$\bar{x}_o = (x_o,y_o,z)$: position vector of the source point

$\bar{x}'_o = (x_o-y_o,z_o)$: position vector of the image of the source point relative to the free surface (z=0)

$H(x-x_o)$: the Heaviside step function which has the property: $H(x) = 0$ for $x \leq 0$

$H(x) = 1$ for $x \geq 0$

The first term is the potential of a unit source in an unbounded fluid. The second and third term account for the presence of the free surface and can be seen as some sort of image system. The second term, or near field disturbance, causes a disturbance symmetrical in x. The third term represents the wave disturbance

trailing behind the source. The full expression is given in Appendix A.

The evaluation of $\phi_1(i,j)$ is basically the same as in the program MICHELL. Only some minor changes were necessary to adapt it to problems at speeds exceeding a Froude number of 0.6. A detailed description of the evaluation of $\phi_1(i,j)$ is given by Raven [24].

In the following, the discussion is limited to the evaluation of the disturbance potential $\phi_2(i,j)$.

The Green's function for the case $z' \neq 0$ $(G_2(\bar{x},\bar{x}_o))$ is better behaved than the Green's function for the two-dimensional problem $(G_1(\bar{x},\bar{x}_o))$. The numerical evaluation is described in appendix A.

Only the waveterm $W(\bar{x}-\bar{x}_o)$ suffers from ill behaviour for $y' = y + y_o \to 0$, and for large values of x' and z'. Aiming at an efficient numerical evaluation, the waveterm has been extensively studied. Firstly analytical reduction of the integral was considered, however, analytical tools were lacking. Next several alternative numerical evaluations were studied. Three of them are discussed in appendix B. Finally, a rather straightforward evaluation was taken, which is only moderately efficient.

As an equidistant grid is used, only multiples of the non-dimensional stepsizes

$$DX = \frac{1}{MM.F_n^2} \text{ and } DY = \frac{T}{L} \cdot \frac{1}{NN.F_n^2}$$

appear as arguments in the Green's function (z' = constant!). Thus, the number of arguments is greatly reduced and this allows an efficient evaluation of the potential $\phi_2(i,j)$.

The term -1/r in the Green's function can now be evaluated beforehand. The range of arguments is:

$-MM.DX \leq x \leq MM.DX$
$-NN.DY \leq y \leq NN.DY$
$z' = \text{constant}$

Because of symmetry the number of evaluations is further reduced and a matrix is filled according to the following expression:

$$R2(m,n) = -\left([(m-1).DX]^2 + [(n-1)DY]^2 + Z'^2\right)^{-\frac{1}{2}}$$

for: $m = 1, \ldots MM+1$
$n = 1, \ldots NN+1$

The same procedure is followed in the evaluation of the terms N() and W() of equation 10. Only now x' ranges between 0 and MM.DX and y' between -2.NN.DY and 0 (for negative x'; W(x') = 0 and N(x')= N(-x')).

Arrays N2(m,n) and W2(m,n) are filled in the following way:

$N2(m,n) = N((m-1).DX,(n-1).DY,Z')$
$W2(m,n) = W((m-1).DX,(n-1).DY,Z')$

for $m = 1, \ldots, MM+1$
$n = 1, \ldots, 2NN+1$

The numerical integration now only involves the choice of the proper matrix elements, multiplying the so assembled Green's function with the source density at the point considered and integrating the result by means of the two-dimensional trapezoidal rule.

The perturbation velocities are determined by 4-point Lagrange differentiation of the potentials at the nodal points; $\phi_1(i,j), \phi_2(i,j)$.

$$u1(i,j) = \partial\phi_1/\partial x$$

$$u2(i,j) = \partial\phi_2/\partial x$$

where: u1 - perturbation velocity corresponding to the demihull in isolation.
u2 - perturbation velocity due to the presence of the other demihull.

Perturbation velocities v1, v2 in y-direction are also calculated. They serve merely as a checking device.

The wave resistance (RW) and the wave interference resistance (RWI) follow from numerical integration (Simpson's rule) of the pressure forces in x-direction over the hull's surface (t(x,y)).

$$R_W = 2.\left[\iint_{S_1} \Delta p1 \; . \; 2\frac{\partial t}{\partial x} dxdy\right] \qquad (17)$$

$$R_{WI} = 2.\left[\iint_{S_1} \Delta p2 \; . \; 2\frac{\partial t}{\partial x} \; dxdy\right] \qquad (18)$$

The following substitutions are made:

- from the linearised Bernoulli equation:
  $\Delta p1 = -\rho.u1.U$ and $\Delta p2 = -\rho.u2.U$
- from (15):
  $\frac{\partial t}{\partial x}(i,j) = 2\pi \; . \; SD(i,j)$

Calculation of sinkage and trim

The sinkage and trim are evaluated in a way similar to the wave-resistance calculation. Starting point is the calculation of the vertical force and the moment around the centre of gravity.

$$F_y = - \frac{DDX \cdot DDY}{9} \cdot s^{\Sigma}_{i,j} \Delta p(i,j) \cdot {}^{DZ}/Dy(i,j)]$$

$$M_Z = - (\frac{DDX \cdot DDY}{9}) \cdot s^{\Sigma}_{i,j}[((i-1) \cdot DDX - XG) \cdot \Delta p(i,j) \cdot {}^{DZ}/Dy(i,j)]$$

where:

DDX, DDY	- dimensional stepsizes
$s^{\Sigma}_{i,j}$	- simpson summation over grid
XG	- position of centre of gravity aft of fore perpendicular
$\Delta p(i,j)$	- perturbation pressure: $-\rho U[ul(i,j)+u2(i,j)]$
DZ/DY(i,j)	- derivative of the offsets in y direction.

DZ/DY(i,j) is calculated from splines representations of the hull sections. Use is made of the IMSL routine ICSCCG.
The derivative of the splines representation is taken. Although the splines representation shows some oscillatory behaviour, the values of the derivatives are in better agreement with reality than for a calculation using lagrange differentiation; especially for hard chine hull forms.
The sinkage follows from:

$$\Delta T = -F_y/(\rho.g.AWP)$$

where:

AWP = waterplane area
ΔT = change of draught at centre of waterplane area

The trim follows from:

$$\tau = -(57.296 /(\rho.g .AWPMI))*[M_Z + F_y.(XWP - XG)]$$

where:

τ - trim in degrees
AWPMI - moment of inertia of the waterplane area.
XWP - distance of centre of waterplane area aft of fore perpendicular

AWP and AWPMI are calculated from the hull offsets by means of trapezoidal integration.

2.2 Hydrostatic resistance due to ventilation at the transom

The hydrodynamic modelling of the transom is already incorporated in the waveresistance calculation. Due to the ventilation of the transom, however, the hydrostatic part of the resistance is no longer a higher order quantity. This component is calculated according to the method proposed by Gadd [13] and Chang [4]. It is extensively discussed in the "Athena model group discussion" [2].

Case 1: complete ventilation

When the transom is completely ventilated the hydrostatic resistance is calculated according to the following formula:

$$R_{HS} = -\iint_{AT} \rho.g.y.dA_T$$

Where integration is over the immersed transom area (A_T), which is Froude number dependent.

Numerically, the hydrostatic resistance is calculated according to the following formula.

$$RHS = \rho \cdot g \cdot [AT \cdot (ZCA_T + DTAPP) + B_T \cdot (DTAPP)^2 + (DTAPP)^3 \cdot (DBT/_{DY})/3] \qquad (20)$$

where: A_T - immersed transom area at rest

ZCA_T - distance from centre of immersed transom area to free surface
(both AT and ZCA_T are calculated from the offsets at the stern by means of the trapezoidal rule)

DTAPP - change of transom immersion; derived from calculated sinkage and trim.

DBT/DY - derivative $\partial Z/\partial y$ at the intersection of the transom with the free surface (Z = offset)

This formula is found to be reasonably accurate (error $\leq$ 5%) for current transom stern forms (i.e. transom sterns with only small variations in $\partial Z/\partial Y$). It follows from the above that the effects of transom sterns which are non-immersed under static conditions are not taken into account.

Case 2: partial ventilation

In the speed range where only partial ventilation occurs, the hydrostatic resistance is calculated as a percentage of the hydrostatic resistance calculated according to (20).
For the lower limit ($F_{nT}=F_{vent}$) of the speedrange where complete ventilation takes place, the following expressions were derived (Table I). F_{nT} is the Froudenumber based on the depth of the transom.

$$B/T \leq 2.50 : F_{vent} = 4.95 - 1.2 \cdot B/T$$

$$B/T \geq 2.5 : F_{vent} = 1.95$$

where: B/T = beam-draught ratio at the transom.

The above formulae are rather arbitrary and need revision when more data are available. Furthermore, it is recognized that F_{vent} also depends upon the ratio $AT/_{Ax}$ and the shape of the transom. The very

limited data, however, did not allow the derivation of a more sophisticated expression.

The correction factor is derived as follows:
First it is assumed that the ventilation depth is proportional to the square of the velocity. So,

$$T_V/T_T = (F_{nT}/F_{vent})^2$$

where: T_V - depth of ventilation
T_T - depth of transom

Based on the assumption of a rectangular shape of the transom, the following expression was derived for resistance due to a partially ventilated transom.

$$RHS' = RHS - (1 - (F_{nT}/F_{vent})^2)^2 * RHS \qquad (21)$$

where RHS as given by (20)

2.3 Skin friction resistance

The following formula is used in the estimation of the skin friction resistance.

$$R_{FR} = \tfrac{1}{2}.\rho.g.U_\infty^2.S_w.(1+\alpha.k_p)(C_{FR}+C_A)$$

where:
U_∞ - free stream velocity
S_w - wetted surface at rest (without transom area)
C_{FR} - 1957 ITTC-skin friction coefficient
C_A - correlation allowance coefficient
k_p - partial form factor
α - 1.5 for transom sterns ($A_T \neq 0$)
2.0 for cruiser sterns ($A_T = 0$)

The partial formfactor (k_p) is calculated analytically according to the formula given by Dawson [7].

$$k_p = \left[\frac{\iint (U/U_\infty)^{3.8} \, dS}{\iint dS}\right] \cdot 856_{-1}$$

where the integration is over the ship's surface and U/U_∞ is the ratio of the local velocity in x-direction to the free stream velocity. Use is made of the velocity distribution calculated with the thin ship theory. This velocitiy distribution includes velocities generated by the second demihull at the location of the first, thus part of the body interference is accounted for in this formfactor. The factor α is necessary to account for the inaccuracy of this simple formula. The specific values are given by Dawson [7]. The difference between the value for transom stern hulls (α=1.5) and the value for cruiser stern hulls (α=2.0) accounts in a simple way for the effect of boundary layer separation on the visous resistance. This effect is not present in the case of transom stern hulls.

It is noted that the effect of the tunnel height on the frictional resistance is not dealt with. Solid water may be present between the demihulls in case of low tunnel heights, thus leading to an increase of the skin frictional resistance (Sherman et al. [27]). Due to the thin ship approach it is not possible to develop an accurate representation of the Froude number dependent part of the viscous resistance (sinkage and trim, wave profile).

2.4 Omitted resistance components

The following resistance components are not included in the resistance model:

- R_{wb} - wavebreaking resistance
- R_{ind} - induced drag
- R_{spray} - spray drag

These components are assumed to be of minor importance. For completeness, they are briefly discussed in the following.

Wavebreaking resistance

When in the wave pattern local values of wave steepness become excessive, waves are no longer stable and will break, thus dissipating wave energy into turbulence. For semi-planing catamarans, two types of wavebreaking are predominant:
(1) wavebreaking due to wave interference and (2) stern wavebreaking. Bow wave breaking is not likely to occur as the bow forms are very fine.

- The superposition of the diverging bow waves may result in a breaking wave between the demihulls. At high Froude numbers or at low hullspacings, wavebreaking may become extreme and lead to additional tunnel wetting thus further increasing viscous resistance.
- Stern wavebreaking: some distance aft of the transom a divergent breaking wave system is initiated by the vortical fluid motion near the free surface. This vortical fluid motion can be associated with two vortices trailing from the stern (Baba [3]).

Wavebreaking depends on the hullform and the hullspacing. The effects of wavebreaking on the resistance cannot be approximated by means of simple analytical tools (e.g. thin ship theory), as it is a non-linear phenomenon. Therefore, it could not be incorporated in the resistance model.

Induced drag

Induced drag arises from trailing streamwise vortices and is thus associated with vessels which generate hydrodynamic lift.
As buoyant forces are predominant the induced drag associated with the planing behaviour is thought to be small in the speedrange considered (Savitsky and Dingee [26]).

The induced drag associated with the asymmetrical properties of the flow depends on the hullform, the aspect ratio (T/L_{WL}) and the hullspacing. The order of magnitude is unknown. It is thought, however, that at very low hullspacings the induced drag may be of importance. A calculation method for the induced drag could not be developed.

Spray drag

High local pressure gradients near the intersection of the bow with the free surface (spray root area) cause the formation of spray. Two kinds of spray can be discerned: blisterspray and whisker spray.
Blisterspray is a thin sheet of water thrown away to the sides and rear of the ship. Under certain conditions the blisterspray may become unstable and break up into droplets; the whiskerspray. The type and extend of spray which is generated is mainly dependent on the Weber number, the Froude number and the bow geometry (Latorre [16]).

Spray drag is composed of a pressure- and a viscous component. The pressure component results from the pressure distribution in the spray root area, while the viscous component is associated with the tangential stresses between the spray and the hull surface. The viscous component may be large when thrown off spray reattaches with the hull or with the connecting structure between the demihulls.

The pressure component of the spray is thought to be small as the fine bow forms result in small pressure gradients. The viscous component will be small when proper spray deflection is applied.

Computation of the spray drag is difficult as both the processes in the spray root area as well as the viscous stresses between the spray and the hull are not well understood. Usual boundary layer equations do not apply to the viscous process in the spray.

3. RESULTS

The program CATRES was subjected to an extensive testing and validation study. Its purpose was to obtain specific information concerning:

- the predictive capability
- the effects of the grid dimensions upon the results
- the execution time
- the restrictions of the method

Major results from this study are discussed in the following.

3.1 Predictive capability

The resistance prediction method was applied to five specific catamaran configurations:*)

1. model A - hull spacing: S/L = .3
2. model A - hull spacing: S/L = .2
3. model B - hull spacing: S/L = .3
4. model B - hull spacing: S/L = .5
5. model C - hull spacing: S/L = .323

The models have the following characteristics (Table II):

- model A: mathematical hull form, symmetrical about the midship section
- model B: derived from a mathematical hull form, featuring conventional propeller arrangement and a small transom stern
- model C: complicated hardchine hull form with a large transom and flat Vee sections along the run.

---

*) Note: models A, B and C were tested at NSMB, however, reports are under proprietary

The study of the predictive capability concentrated on:

- the accuracy of the prediction of the total resistance
- the accuracy of the prediction of each resistance component
- the accuracy of the prediction of the sinkage and trim

The results are discussed in the following

Total resistance (R_T)

Figs. 9 through 13 show the results of the resistance calculations together with extrapolated modeltest results. The results of the resistance calculations consists of both values for the total resistance and values for the seperate resistance components.

Modeltest results were extrapolated by the usual Froude method, with the skin friction coefficients determined by the '57 ITTC-line. In the extrapolation of modeltest results, the correlation allowance coefficient (C_A) was taken .0003 for models A and B and C_A = .0004 for model C. Corresponding values for C_A were used in the program CATRES. Calculations were made with griddimensions (MM x NN) of 20 * 6 for model A and 20 * 10 for the models B and C.

At the very low hullspacing: S/L_{WL} = 0.2, the resistance of model A is greatly underpredicted at Froudenumbers greater than .5 (Figure 9). The underestimation amounts to about 20% of the measured resistance. This discrepancy is thought to be mainly composed of induced drag. Comparison of photographs taken during modeltesting with the ones taken at larger hullspacings did not show major differences in spray and wavebreaking phenomena.

For the four other cases ($S/L_{WL} \geq .3$; Figs. 10-13), the correlation is very good for: $.5 \leq Fn \leq 1.0$. The mean error is: $\bar{x} = -3.7\%$ with a standard deviation: $s = 5.3\%$.

For the models A (S/L_{WL} = 0.3 only) and B (Figs. 10, 11 and 12), the underprediction of the resistance is consistent. The discrepancy starts to increase at speeds exceeding Fn =0.8. The steadily increasing error is mainly due to spray and wavebreaking. Photographs reveal that wavebreaking is present at Fn = 0.8 and that the visual phenomenon develops steadily. Observations also show that the development of spray grows rapidly at speeds in excess of Fn = 0.8. At Fn = 1.15 large sheets of spray (blister spray) are present. Most of the blister spray is attached to the hull. It is thought that the viscous forces between blister spray and the hull give a major contribution to the spray drag. The models A and B were not fitted with spray deflection strips, unlike model C (Fig. 13) which is a hardchine hull form showing effective spray deflection. Photographs do not show pronounced spray or wavebreaking phenomena for this model.

It is clear that the resistance model cannot adequately handle special cases characterised by pronounced wavebreaking, spray and/or large values of induced drag. It should be noted, however, that models A and B are not characteristic for current designs. Furthermore a hullspacing smaller than a quarter of the length is exceptional.

It is concluded from the results that the differences in the resistance characteristics of the models are fairly well predicted. This is an important matter as it allows for an evaluation of major resistance differences ($\geq$ 10%, approximately) between catamaran-designs.

Figure 14 shows for all five cases the wave interference factor IF_{wp} as a function of the Froude number. As was expected, the maximum value tends to decrease with increasing AT/A_x-ratio.

Resistance components

Although the prediction of total resistance is rather good and consistent, the question remains whether or not the separate resistance components are accurately predicted or not.

First, the correctness of the calculation of the waveinterference resistance has been checked. At Froude numbers between values 0.3 and 0.4, waveresistance calculations were made for the mathematical hull form defined by:

$$z/B = (1 - (x - L_{WL}/_2)^2/(L_{WL/2})^2).(1 - y^2/T^2)$$

where: z/B-dimensionless offsets.
The results are compared with data provided by Everest [10] (see Fig. 18). A perfect fit with other thin ship results is shown. The phase difference with measured results is characteristic for thin ship calculations. It results from the fact that, within the thin ship theory, the apex of the Kelvin pattern coincides with the stem. In reality it is located somewhat forward of the stem, resulting in an outward translation of the Kelvin pattern.

As mentioned before, a basic assumption of the method is that the difference in hydrodynamic (wave-) resistance between a fixed model and a model free to sink and trim is only small. Calculations were made in order to get an impression of the reliability of this assumption.
Two sets of input were prepared for the hard chine hullform (model C):

1. input corresponding to the fixed model; without sinkage or trim
2. input corresponding to the model placed in the measured equilibrium position; initial sinkage and trim

Calculations at Fn=0.9 gave the following results:
case 1: total waveresistance (RW + RWI)= 4.7 KN
case 2: total waveresistance = 2.7 KN
(see also Tables III and IV). This large difference between the two

figures leads to the conclusion that the assumption mentioned above is doubtfull.

Assuming that the modelling of the transom is correct, the hydrostatic resistance component can be checked. Figures 15, 16 and 17 show the predicted values for the hydrostatic resistance component (only models B & C), together with values derived from sinkage and trim measurements (transom immersion). The correlation between both datasets is only moderate. At high speeds (F_n>0.7) this resistance component is appreciably overpredicted which is due to an overprediction of the transom immersion. Later on we will return to the prediction of transom immersion (sinkage and trim).

The correctness of the model for the frictional resistance could not be checked. Although the calculated form effect seems to improve the correlation in the hump speed range, the significance of the form effect is too small to allow definite conclusions. It was found that interference effects can double the form effect, and that the form effect is only significant at speeds between Fn=0.4 and Fn=0.6 (Figs. 9,10,11).

sinkage and trim

As the prediction of the transom immersion was found to be poor for two models (Figs. 16, 17), the calculation of sinkage and trim was suspected of inaccuracies. Figs. 19 through 24 show for all models the predicted and measured values for sinkage and trim.
It is thought that there are two main causes for the inaccurate predictions:

- thin ship theory cannot cope with hulls developing positive hydrodynamic lift as the calculations are made for the case of zero trimangle (fixed model). Moreover, an iterative scheme for finding the equilibrium position cannot be followed, as this is not consistent with the basic thin ship assumption of a small disturbance.

- an inaccurate calculation of the vertical force and the trimming moment.

The latter cause was studied a little further. For model C input was prepared appropriate to the equilibrium position found by experiments (Fn = .9; rise of CG: +0.07 m; trim 1,15^{o}). Calculations were made for several combinations of grid dimensions (MM,NN). The results are shown in Table III. They are rather disappointing, with large variations in trim and rise of CG (thus R_{HS}). These inconsistencies may be due to an inaccurate hull representation due to the disconinuity in the derivatives of the frames in vertical direction. These derivatives are used in the integration of the vertical components of the pressure forces. Furthermore, it should be mentioned that model C has extreme low deadrise angles near the stern (4 at the aft perpendicular).

3.2 Effects of the grid dimensions upon the results

The grid dimensions MM and NN are important parameters as they affect both the accuracy, and the execution time. A limited study was made of the effects of the grid dimensions upon the results. It was found that the accuracy is affected by:

- the dimensions of the panels relative to the dimensions of the waves
- the hullform

The effects of the hullform were studied more closely; the tendencies found are discussed in the following.

The effects of the hullform seems to be only present for hard chine hullforms. For more conventional shapes there is a good convergence of the results when the number of panels is increased.
For the hard chine hullform it appeared that the values for the trim and sinkage are most sensitive to a variation of the grid dimensions (Tables IV, V). The other resistance components (RT-R_{HS}) show only small variations with the grid dimensions. The results for R_{HS}, trim and sinkage depend most of all upon the number of

panels in vertical direction, suggesting large differences in the hull representation (derivatives of the frames in vertical direction). It is thought that this typical behaviour for model C is partly due to the extremely low deadrise angles near the stern.

3.3 Execution time

The execution time needed for running the program CATRES is about 2-3 times larger than the one for the program MICHELL. The latter program computes only the wave resistance of a monohull. The execution time depends on the hullform, the hullspacing, the length-draught ration and the Froudenumber range. At this stage only rough indications can be given. For a hardchine hullform, requiring a rather dense grid in both horizontal and vertical direction (MM=20, NN = 10), about 400 CP seconds are needed for 10 resistance evaluations in the interval: $.3 \leq Fn \leq 1.0$. This figure may decrease to about 100 CP seconds for a more conventional hullform. No special efforts were taken in program optimization.

3.4 Restrictions

During the testing of the program CATRES indications were found for the following restrictions to the applicability of the program.

- due to the thin ship approach, the length-beam ratio should be large: i.e. $L/B > 8.0$
- hullspacings should be larger than a quarter of the length
- the hydrodynamic lift should be small: i.e. $L_{HD} \leq .2\text{-}.3$
- for hard chine hulls the deadrise angle should be larger than 10 - 15 degrees

4. FINAL REMARKS

The resistance prediction method for semi-planing catamarans (program CATRES), is found to be a valuable tool for the evaluation of the bare hull resistance of catamarans with symmetrical demihulls. The method can be applied to a variety of hullforms, ranging from mathematical hullforms to hardchine hullforms, although representation of hardchine hullforms is still a point of concern. Testing of the program revealed that, within the following restrictions:

- Fn $\leq$ 1.0
- moderate to large hull spacings: $S/L_{WL} \geq .25 - .30$.

the correlation between predicted total resistance and four sets of modeltest data is very good (i.e. for $0.5 \leqslant Fn \leqslant 1.0$, a mean error of -3.7% and a standard deviation of 5.3% was found).
The execution time for running the program is moderate. In general less than 40 CPU seconds per Froudenumber are required for a hard chine hullform. For more conventional hullforms this figure may decrease to about 10 CP seconds per Froudenumber.

Main conclusions are

- the method can be used for the evaluation of main differences in resistance characteristics (> 10% approximately) of different catamaran designs
- the calculation of the waveinterference resistance is accurate. The results show a perfect fit with results from another thin ship method.
- within the restrictions, as given above, the limited resistance model proves to be sufficient for modelling the resistance of semi-planing catamarans.
- the implicit assumption of small differences between the hydrodynamic resistance of a fixed and a free floating model is doubtfull for hardchine hullforms at high Froudenumbers (Fn≈1.0).
- representation of hard chine hullforms can be inaccurate; especially when the hull has very low deadrise angles.

Points of further study:

- the representation of hard chine hullforms. These hullforms are characterised by a discontinuity in the hull derivatives at the chines which leads to an inaccurate integration of pressure forces.
- the case of asymmetric demihulls. The camber of these hulls may be represented by a doublet distribution. It is noted however that severe numerical problems are expected.

List of references

1. Allema, J.H.: "A study of two computerprograms for the resistance prediction of SWATH ships", NSMB Report No. 43755-4-DR, Febr. 1982.

2. Athena Model Group Discussion, Proceedings of the workshop on ship wave resistance computations, Vol. 1, DTNSRDC, Bethesda, Nov. 13-14, 1979, pp. 75-85.

3. Baba, E.: "Wavebreaking resistance of ships", Soc. Nav. Arch. of Japan, International seminar on wave resistance, Session II-2, Tokyo, Febr. 3-5, 1976.

4. Chang, M.S.: "Wave resistance predictions by using a singularity method", Proceedings of the workshop on ship wave resistance computations, DTNSDRC, Bethesda, 1978, pp. 202-214.

5. Chapman, R.B.: "Hydrodynamic drag of semi-submerged ships", Trans. ASME, Vol. 4, 1982, pp. 879-884.

6. Clement, E.P.: "Graphs for predicting the ideal high speed resistance of planing catamarans", David Taylor Model Basin, Report No. 1573, Nov. 1961.

7. Dawson, C.W.: "Calculations with the XYZ Free Surface program for five ship models", Proc. of the Workshop on Ship Wave Resistance Computations, DTNSRDC, Bethesda, 1978, pp. 232-255.

8. Eggers, K.: "Uber Widerstandsverhältnisse von Zweikörperschiffe", Jahrbuch der Schiffbautechnischen Gesellschaft, 49, 1955.

9. Eggers, K.: "Über die Ermittlung des Wellenwiderstandes eines Schiffsmodels durch Analyse seines Wellensystems", Schiffstechnik, Bd. 9, 1962.

10. Everest, J.T.: "Some Research on the hydrodynamics of catamarans and multi-hulled vessels in calm water", Trans. N.E. Coast Inst. of Engineers and Shipbuilders, Vol. 84, 1968, pp. 129-147.

11. Everest, J.T. and Bailey, D.: "The Wave Resistance of High Speed semi-displacement type hulls and its influence on the design of unconventional high speed craft", Contribution to the panel discussion, 7th Symp. on Naval Hydrodynamics, ONR, Rome, 1968 (see panel disc. in proc. of 7th Symposium).

12. Fry, E.D. and Graul, T.: "Design and application of modern high speed catamarans", Marine Technology, July 1972, pp. 345-357.

13. Gadd, G.E.: "Contribution to the Workshop on Ship Wave Resistance Computations", Proc. of the Workshop on Ship Wave Resistance Computations, DTNSRDC, Bethesda, Nov. 1978, pp. 117-161.

14. Hess, J.L. and Smith, A.M.O.: "Calculation of nonlifting potential flow about arbitrary three dimensional bodies", Douglas Aircraft Company, Report No. 40662, March 1962.

15. Kusaka, Y. et al: "Hull form design of the semi-submerged catamaran vessel", 13th Symp. on Naval Hydrodynamics, Session V-5, Tokyo 1980.

16. Latorre, R.: "Study of prismatic planing model spray and resistance components", Journal of Ship Research Vol. 27, Sept. 1983, pp. 187-196.

17. Lin, W.C.: "The force and moment on a twin-hull ship in a steady potential flow", 10th Symp. on Naval Hydrodynamics, 1974, pp. 493-516.

18. Lunde, J.K.: "On the linearized theory of wave resistance for displacement ships in steady and acceleration motion", Trans. SNAME, Vol. 59, 1951, pp. 25-74.

19. Maruo, H.: "High- and low aspect ratio approximations of planing surface craft", Schiffstechnik, Bd. 14, 1967(72), pp. 57-64.

20. Michell, W.H.: "The seagoing catamaran ship its features and its feasibility", Int. Shipb. Progress, Sept. 1961.

21. Noblesse, F.: "The fundamental solution in the theory of steady motion of a ship", Journal of Ship Research Vol. 21, No. 2, June 1977, pp. 82-88.

22. Oving, A.J.: "Semi-planing catamarans; study of resistance and resistance prediction", interimreport,april 1985.

23. Pien, P.C.: "Catamaran hull form design", Int. Sem. on Wave Resistance, Session V-2, Tokyo, Febr. 1976.

24. Raven, H.C.: "Calculation of wave profile and waveresistance by the thin ship theory; the first order problem", NSMB Report No. 50002-1-SR, Nov. 1980.

25. Savitsky, D.: "Hydrodynamic design of planing hulls", Marine Technology, Oct. 1964, pp. 71-95.

26. Savitsky, D. and Dingee, D.A.: "Some interference effects between two flat surfaces planing parallel to each other at high speed", Journ. of Aeronautical Sciences, 1954(21), No. 6. pp. 419-420.

27. Sherman, J. and Fisher, P.: "A study of planing catamaran hull and tunnel interactions", The University of Michigan, Ann Arbor, Febr. 1975.

28. Tanaka, H. et al: "Study on design of catamaran hull form with asymmetric demihulls", Ship Research Institute of Japan, (16)1979, Report No. 4.

29. Tasaki, R.: "A note on wavemaking resistance of catamarans", Technical Report, the university of Michigan, Ann Arbor, Oct. 1962.

30. Tattersal, E.G. and Hons, D.L.C.: "The HM500 series of sidewall hovercraft", Naval Architect, Febr. 1985, pp. 53-68.

31. Tulin, M.P.: "The theory of slender surfaces planing at high speeds", Schiffstechnik, Bd. 4, 1957(21), pp. 125-133.

32. Wang, D.P. and Rispin, P.: "Three-dimensinal planing at high speeds", Journal of Ship Research, Sept. 1971, pp. 221-230.

Appendix A:

Calculation of the unit source potential or Green's function; (three-dimensional case: $z' \neq 0$).

After Noblesse [21], the unit source potential for the case $z-z_o \neq 0$ can be written as follows:

$$(16) \qquad G(\bar{x}; \bar{x}_o) = -1/r + N(\bar{x} - \bar{x}_o') + H(x - x_o).\, W(\bar{x} - \bar{x}_o')$$

where:

$x = (x, y, z)$: position vector of the field point

$x_o = (x_o, y_o, z_o)$: position vector of the source point

$x_o' = (x_o, -y_o, z_o)$: position vector of the image of the source point relative to the free surface ($y = 0$).

$H(x - x_o)$: the Heaviside step function, which has the property:

$H(x) = 0$ for $x \leq 0$.

$H(x) = 1$ for $x > 0$.

Further, the following notation is introduced:

$$(\bar{x} - \bar{x}_o') = (x', y', z').$$

$$r = \sqrt{[(x-x_o)^2 + (y-y_o)^2 + (z-z_o)^2]}$$

$$r' = \sqrt{[x'^2 + y'^2 + z'^2]}$$

Now, the full expressions for the near field and wave-disturbance can be written as follows.

$$(A\text{-}1) \qquad N(\bar{x} - \bar{x}_o') = {}^{1}/_{r'} - 2.\left[1 + \frac{-y'/r'}{1 + \|x'\|/r'}\right] + \frac{2}{\pi}\int_{-\pi/2}^{\pi/2} \mathrm{Im}\left[e^{Z}.E_1(Z) + \ln Z\right] \cos\theta\, d\theta$$

with $E_1(Z)$ - the exponential integral: $\int_Z^\infty \frac{e^{-t}}{t}\, dt$

and $Z = [(y'\cos\theta + z'\sin\theta) + i\|x'\|] \cos\theta$

(A-2)

$$W(\bar{x} - \bar{x}'_o) = -4 \cdot e^{y'} \int_{-\infty}^{\infty} e^{y't^2} \cdot \sin\left[(x' + z't)\sqrt{(1+t)^2}\right] dt; \quad y' \leq 0$$

As $z' \neq 0$, the first term $(-1/r)$ is regular for all x' and y' and can easily be evaluated.

Near field disturbance: $N(\bar{x} - \bar{x}'_o)$

All three terms of the near field disturbance are regular. The first and second term are evaluated as in (A-1). The third term is evaluated according to formula's given by Noblesse [21]. The treatment is similar to the one in MICHELL for the two-dimensional case ($z' = 0$).

The function $E_1(Z)$ can be easily and effectively evaluated as both an ascending series and an asymptotic expansion are available. Substitution of the ascending series for $E_1(Z)$ permits the integrand of the third term of (A-1) to be written as follows (Noblesse [21], formula 21b).

$$e^Z E_1(Z) + \ln Z = -\gamma - \sum_{n=1}^{\infty} \left(\ln Z + \gamma - \sum_{m=1}^{n} \frac{1}{m}\right) \frac{Z^n}{n!}$$

where: γ = Eulers constant

The imaginary part should be taken, therefore we substitute:

$$Z = \rho \cdot e^{i\varphi}$$

where: $$\rho = \left[(y'\cos\theta + z'\sin\theta)^2 + (x')^2\right]^{\frac{1}{2}} \cdot \cos\theta$$

$$\varphi = \text{arctg}\left[\frac{\|x'\|}{y'\cos\theta + z'\sin\theta}\right]$$

which yields,

(A-3) $$\mathrm{Im}\left[e^{Z}.E_1(Z) + \ln Z\right] =$$

$$= \sum_{n=1}^{\infty} \left[\frac{\rho^n}{n!}\left(\phi.\cos(n.\phi) + \left(\ln\phi + \gamma - \sum_{m=1}^{n}\frac{1}{m}\right)\sin(n.\phi)\right)\right]$$

Although the expressions for ρ and ϕ are different, the overall expression is equivalent to the one for the 2-dimensional case. The expression is valid for $0 \leq r' \leq \infty$, but for large values of r', it is not a practical means of computation.
The expression is only used for small to moderate values of ρ ; i.e. $\rho \leq 15$.

For values of ρ exceeding 15, the asymptotic expansion is used, yielding:

$$e^{Z}E_1(Z) + \ln Z = \ln Z + \frac{1}{Z} + \sum_{n\geq 1} (-1)^n.\frac{n!}{Z^{n+1}}$$

Substituting once again $Z = \rho.e^{i\phi}$, the following expression is obtained:

(A-4)

$$\mathrm{Im}(e^{Z}.E_1(Z)+\ln Z) = \phi - \frac{1}{\rho}.\sin\phi - \sum_{n\geq 1}\frac{(-1)^n.n!}{\rho^{n+1}}.\sin(n+1).\phi$$

For $x' \neq 0$ the integrand is evaluated according to (A-1) or (A-2) (FUNCTION TERMINT 2). The integral is obtained by numerical integration (simpson's rule) with a step size of $\pi/32$. (NGREEN2).

For $x' = 0$, $N(\bar{x} - \bar{x}'_o)$ is written as:

$$N(\bar{x}') = Q(\bar{x}')/r'$$

where: $$Q(\bar{x}') = 1 + \sum_{n=1}^{\infty}\frac{(-1)^n\, 2^{n+1}.\rho'^{,n}}{1.3\ldots.(2n-1)} \quad ; \quad 0 \leq \rho' \leq \infty$$

$$\rho' = (r' - y')/2$$

Wave disturbance: $W(\bar{x} - \bar{x}'_o)$

$$W(\bar{x} - \bar{x}'_o) = -4.e^{y'} \cdot \int_{-\infty}^{\infty} e^{y't^2} \cdot \sin\left[(x' + z't)\sqrt{(1 + t^2)}\right]dt;\ y' \leq 0$$

This expression is extremely tedious. The integral is characterised by singular behaviour for $y' \to 0$, causing the integrand to be non-zero over the whole range of integration. Furthermore, the integrand is ill behaved for large values of x', z', for which it is highly oscillatory. Both properties prohibit a straightforward evaluation of the wave disturbance term.
Extensive study has been made of the wave disturbance term, aiming at an efficient numerical evaluation (Appendix B). The result of this study is not fully satisfactory as the numerical method which was finally adopted is rather brute-force and neither elegant nor efficient.

For all $x', y' \neq 0$ the wave disturbance is computed by direct numerical integration using simpson's rule (subroutine WSIMP). Note that for $x' = 0$ the integrand is anti-symmetric in t, consequently; $W(\bar{x}') = 0$.
As the oscillatory character of the integrand depends on the values of x', z', the step size is related to these parameters as follows:

- initial stepsize ($t = 0$):
$$H_o \leq \frac{\pi}{10} \cdot 1/(.001 + x + 5 \cdot \|z'\|)$$
- further; ($t \neq 0$):
$$H \leq \frac{\pi}{10} \cdot 1/(.001 + x + 2 \cdot \|z'\|.t)$$

Resulting in at least 20 function evaluations per period of the sinus-term.
To obtain a uniform error in the integration it was necessary to reduce the stepsize to $H_o/3$, $H/3$ respectively for $x' \leq 3$. and $z' \leq 2$. This approach resulted in an absolute error less than 1.10^{-6}.

A secondary error arises from termination of the integration at some value t=TSTOP. This error was set to about 1.10^{-6} by taking:

(1) for: $x' \leq 1.5$; $z' \leq 1.$ & $y' \geq -.2$: $TSTOP = \sqrt{\left\| \frac{ALOG\ (10^{-6})}{y'} \right\|}$

(2) else : $TSTOP = \sqrt{\left\| \frac{ALOG(10^{-5})}{y'} \right\|}$

The total absolute error in the value of $W(\bar{x}')$ is smaller than 1.10^{-5}.

The values of $W(\bar{x}')$ for $y' = 0$ are obtained from the values of $W(\bar{x}')$ for $y' \neq 0$ by 3 point lagrange extrapolation. Although there is no mathematical justification of this method, it proved to give a sufficient accuracy (see Appendix B).

Appendix B

Study of numerical evaluations of the wavedisturbance: $W(\overline{x}')$. (three-dimensional case: $z \neq 0$).

Subject is the wavedisturbance term:

$$W(x',y',z') = -4.e^{y'} \int_{-\infty}^{\infty} e^{y't^2} . \sin[(\bar{x}' + z't).\sqrt{1 + t^2}]\,dt$$

with $x' \geq 0$; $y' \leq 0$.

Preliminar investigations revealed two main problems:

1. the ill-behaviour of the integrand for $y' \to 0$, prohibiting a straightforward numerical evaluation of $W(\bar{x}')$ at $y' = 0$.
2. straightforward numerical integration of the integrand is very inefficient for small values of $\|y'\|$; $\|y'\| \leq 0.1$.

Consequently several alternative methods of evaluation were studied aiming at an efficient evaluation of $W(\bar{x}')$ for small values of $\|y'\|$. A brief discussion of a number of alternatives is given in the following.

Three-dimensional polynomial representation

A three-dimensional representation of the integral by means of Tsjebysjev polynomials was sought. This approach would only require one large initial investment for the determination of the Tsjebysjev coefficients. Subsequent evaluations are efficient and follow from the next formula:

$$W(x'', y', z'') = \sum_{k=1}^{K} \sum_{l=1}^{L} C_{kl}(y').T_k(x'').T_l(z'')$$

where: x'', z'' : coordinates x', z' transformed to the interval $(-1, 1)$.

$C_{kl}(y'')$: the Tsjebysjev coefficients as function of y'.

T_k, T_l : Tsjebysjev polynomials.

The Tsjebysjev coefficients follow from:

$$C_{kl}(y') = \frac{1}{\|T_k\|^2} \cdot \frac{1}{\|T_l\|^2} \cdot \int_{-1}^{1}\int_{-1}^{1} \frac{1}{\sqrt{1-x''^2}} \cdot \frac{1}{\sqrt{1-x''^2}} \cdot T_k(x'') \cdot T_l(z'') \cdot W(x'',z'') \cdot dx''.dz''$$

where: $W(x'',z'')$ may be given in tabular form.

Initial studies were made concerning one dimensional representations of $W(\bar{x}')$, (along lines in planes y' = Constant). The region considered, was bounded by the following restrictions:

$.25 \leq F_n$

$.15 \leq S/L_{WL} \leq .6$

which led to: $16 \geq x' \geq 0$; $.15x' \leq z' \leq 10$.

The restriction $z' \geq 15.x'$ leads to the exclusion of a region with strong oscillations (Fig. B-1).

From these one-dimensional studies it was found that polynomial representation is unfeasible. It was estimated that the initial investment would be at least some 100.000 CP seconds execution time.

In the region with only small changes in $W(\bar{x}')$, (outside Kelvin pattern; see Fig. B-1), polynomial representation may still be a reasonable alternative. Due to time limits however, no further studies could be undertaken.

Direct numerical evaluation (Simpson's rule)

The main problem in direct calculation is the evaluation of $W(\bar{x}')$ at the singular points y' = 0. Two methods for evaluation of W(x',0,z') were tested.

First, the problem at y' = 0 may be solved by writing:

$$W^*(\bar{x}') = -4.e^{y'} \int_{-\infty}^{\infty} \frac{e^{y't^2}}{(1+t^2)} \cdot \sin\left[(x'+z'.t).\sqrt{(1+t^2)}\right] dt$$

Where the following relation holds: $\frac{\partial W^*(\bar{x}')}{\partial y'} = W(\bar{x}')$

$W^*(\bar{x}')$ is regular and can be evaluated for $y' = 0$. $W(\bar{x}')$ then follows from $W^*(\bar{x}')$ by numerical differenciation in y'-direction. Three point Lagrange differentiation gave the best results. The evaluation of $W^*(x', 0, z')$ is expensive as the break-off point of the integration needs to be large. The term $(1 + t^2)$ is only slowly decreasing.

From the above it follows that $W(\bar{x}')$ is bounded at $y' = 0$. Therefore the expensive evaluation of $W^*(\bar{x}')$ was circu vented by obtaining $W(x', 0, z')$ by extrapolation from $W(x', y', z')$. Again three point Lagrange differentiation gave the best results.

Both methods were applied to grids characteristic for the Froude numbers 0.3, 0.7, 1.5 ($x'_{max} = F_n^{-2}$). It was found that the first method ($W^*(\bar{x}')$) took between 2 and 5 times more execution time than the simple evaluation by extrapolation. This is due to the evaluation of $W^*(x', 0, z')$. Furthermore the accuracy of the methods was tested numerically by means of the free surface condition:

$$W_{xx} + W_y = 0$$

For the grids appropriate to Fn = 0.3, 0.7, both methods resulted in a comparable accuracy of $W(x',0,z')$. For the grid characteristic for Fn = 1.5 the accuracy obtained by the extrapolation method was much better than the one for the differentation method (difference: 0(10)). Consequently, the extrapolation method was finally adopted in the program CATRES.

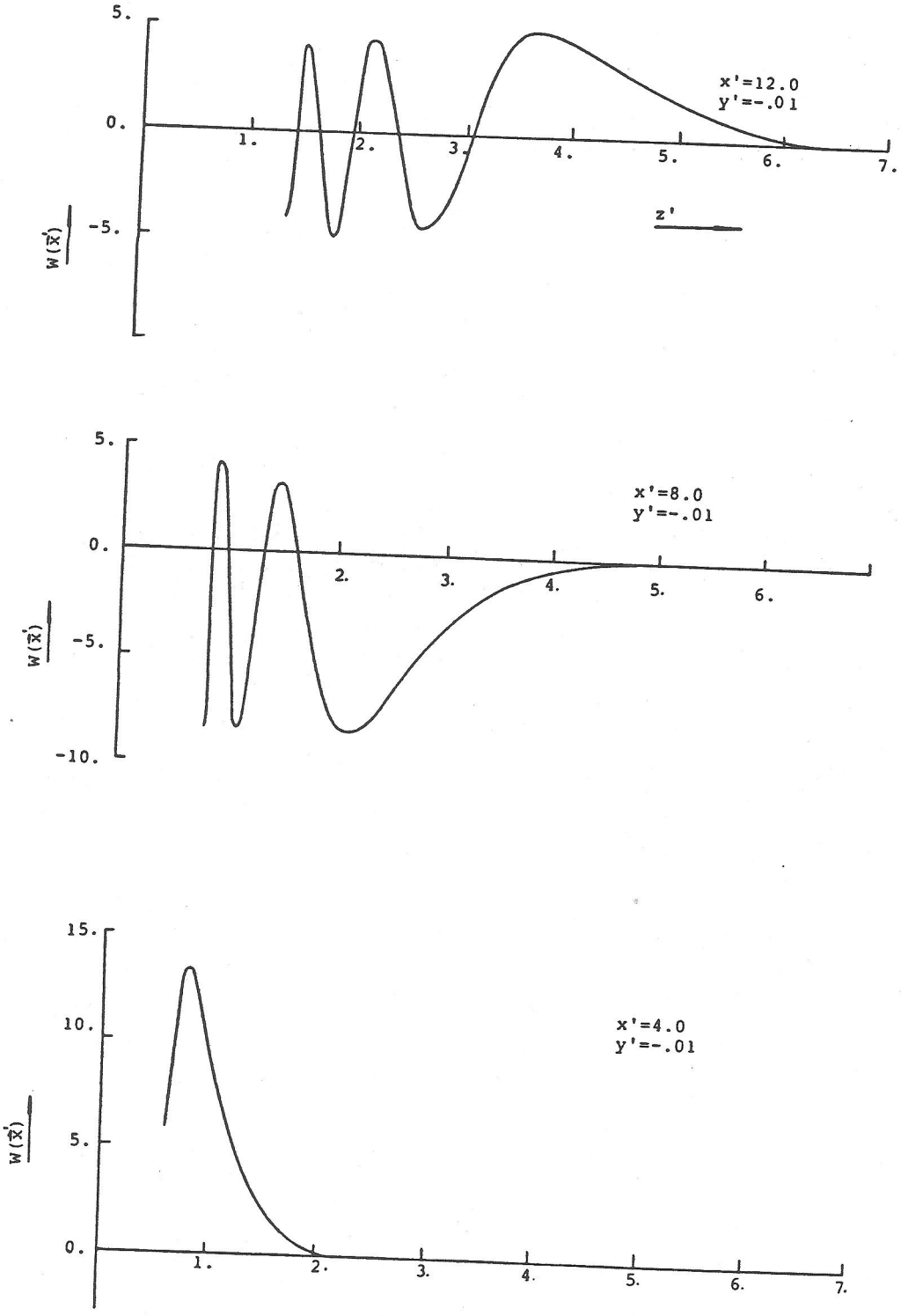

Figure B-1: wavedisturbance term of the Greens function as a function of x' and z'

TABLES

B/T	Fn	F_{nT}	T_V/T_T	remarks
.9	.647	3.04	60 %	-
.9	.810	3.81	100 %	upper limit of F_{vent}
3.28	.380	2.02	100 %	upper limit " "
4.20	.30	1.94	100 %	exact limit " "
4.24	.380	2.3	100 %	upper limit " "
6.62	.380	2.87	100 %	upper limit " "

notes:- F_{nT} = Froudenumber based on the draught at the transom
- T_V = sinkage of free surface behind the transom
- T_T = draught at transom

Table I : dataset used for the determination of the limit of complete ventilation of the transom

1TTC

MODEL	:	A	B	C
LENGTH	:	16.00 m	16.00 m	18.34 m
BEAM	:	2.00 m	2.00 m	2.15 m
DRAUGHT	:	1.50 m	1.50 m	.85 m
WETTED SURFACE	:	53.95 m^2	51.03 m^2	94.52 m^2
∇	:	19.47 m^3	18.13 m^3	27.30 m^3
A_T/A_X	:	0.00	0.153	0.78
C_p	:	.637	.669	--
C_b	:	.406	.378	.407
L/B	:	8.00	8.00	8.53
B/T	:	1.33	1.33	2.53

CA ⇒ 0.0003 0.0003 0.0004

Table II : model characteristics

MM	20	10	6	6
NN	10	10	10	6
RT	22.34	23.945	20.46	23.53
RW	2.614	2.367	2.388	2.518
RWI	.101	.081	.081	.053
RHS	3.59	5.508	2.21	4.95
RFR	16.026	15.989	15.785	16.011
RT-RHS	18.75	18.44	18.25	18.58
TRIM (degr.)	.672	1.49	.595	1.27
RISE OF CG (m)	.027	.038	.106	.036
note: resistances in KN				

Table III: Results for model C as a function of the grid dimensions: Fn=0.9, initial trim and sinkage

MM	20	20	20
NN	6	8	10
RT	24.388	26.395	25.97
RW	4.740	4.643	4.797
RWI	-.066	-.077	-.063
RHS	3.686	5.700	4.895
RFR	16.027	16.128	16.160
RT - RHS	20.702	20.695	21.075
TRIM (degr.)	1.214	1.908	1.493
RISE OF CG (m)	.027	-.002	-.016

MM	10	14	20
NN	10	10	10
RT	25.865	25.973	25.97
RW	4.761	4.842	4.797
RWI	-.074	-.068	-.063
RHS	5.084	5.076	4.895
RFR	16.094	16.193	16.160
RT - RHS	20.781	20.897	21.075
TRIM (degr.)	1.650	1.589	1.493
RISE OF CG (m)	-.001	-.009	-.016

note: resistances in KN

Table IV: Results for model C as function of the grid dimensions (Fn=0.9)

MM	20	20	20
NN	6	10	14
RT	14.207	14.96	15.207
RW	2.915	2.883	2.893
RWI	.500	.515	.515
RHS	4.595	5.425	5.590
RFR	6.196	6.140	6.208
RT - RHS	9.612	9.535	9.617
TRIM (degr.)	1.084	1.369	1.439
RISE OF CG (m)	-.051	-.063	-.062

MM	14	20	26
NN	10	10	10
RT	15.025	14.96	14.996
RW	2.879	2.883	2.896
RWI	.513	.515	.523
RHS	5.442	5.425	5.390
RFR	6.191	6.14	6.188
RT - RHS	9.583	9.535	9.606
TRIM (degr.)	1.378	1.369	1.346
RISE OF CG (m)	-.062	-.063	-.063

note: resistances in KN

Table V : Results for model C as function of the grid dimensions (Fn=0.4)

FIGURES

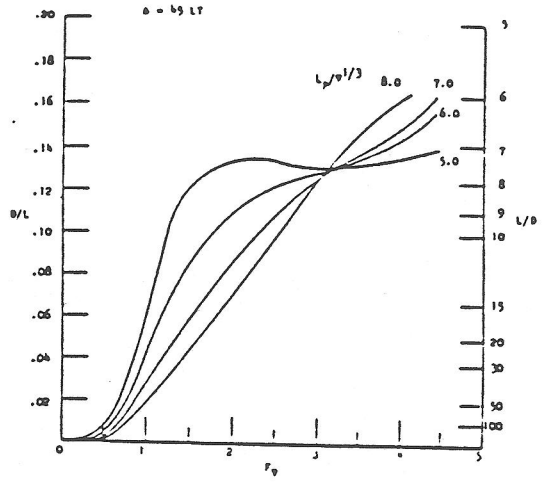

figure 2: Drag/lift ratio for planing hulls as function of volume froudenumber and slendernessratio

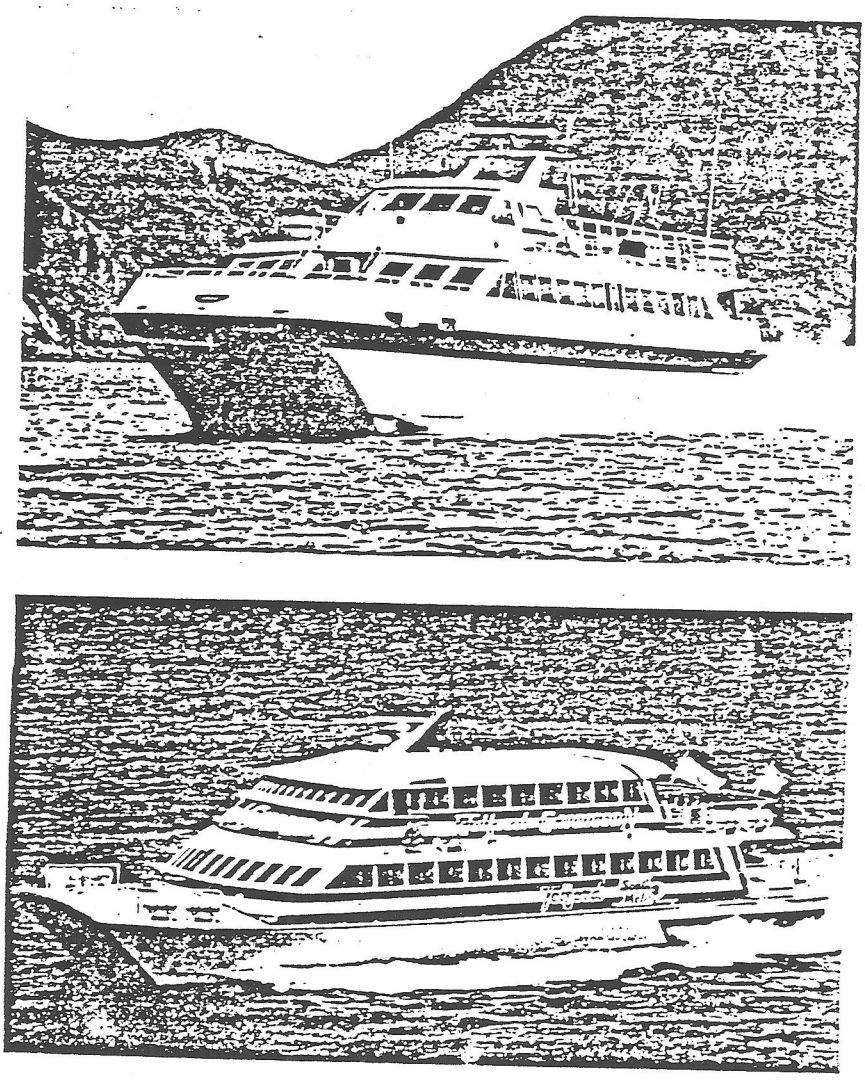

figure 3: recent catamaran-designs

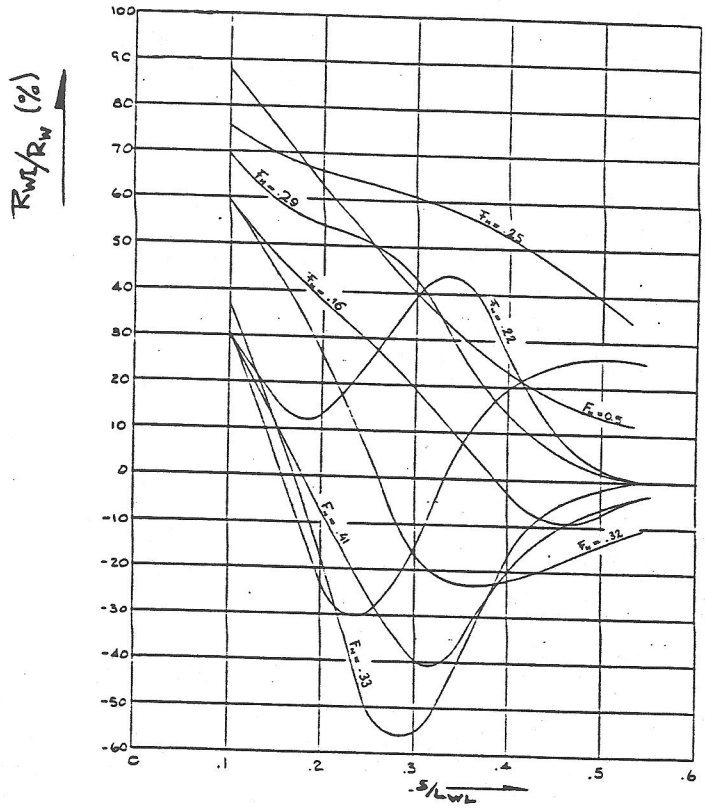

figure 4 : Interferencefactor as a function of hullspacing (source Tasaki [3])

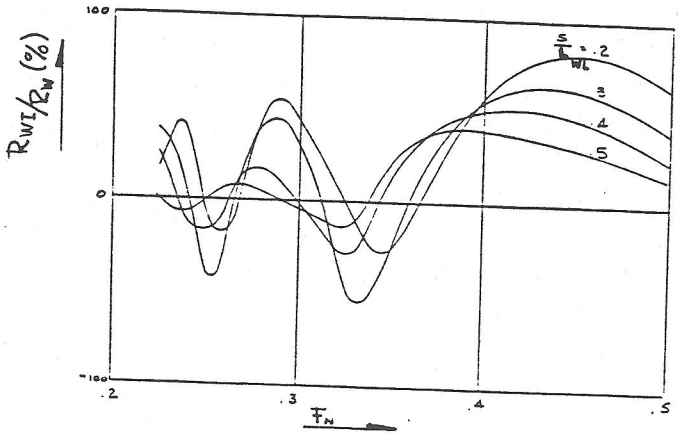

figure 5 : Interference-factor as a function of froudenumber (Tasaki [3])

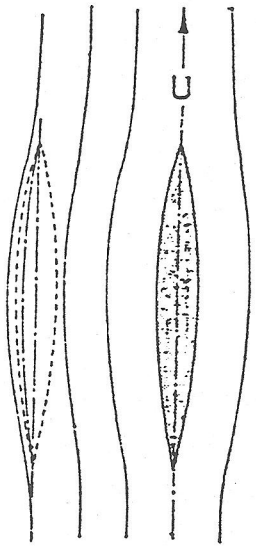

figure 6 : bodyinterference

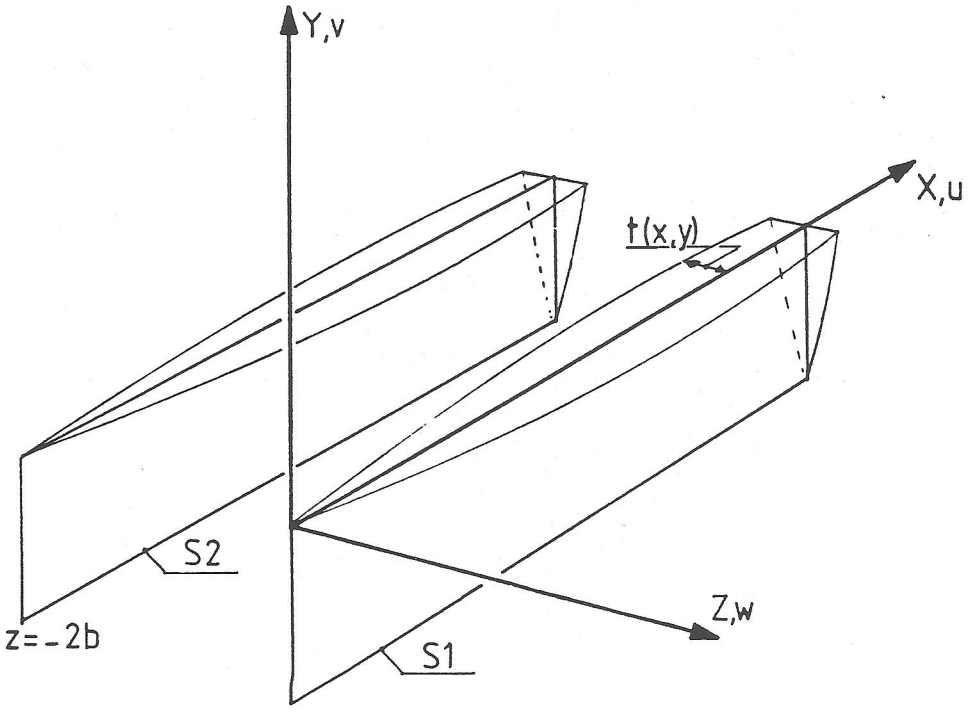

Figure 7: coordinate system of the flowproblem

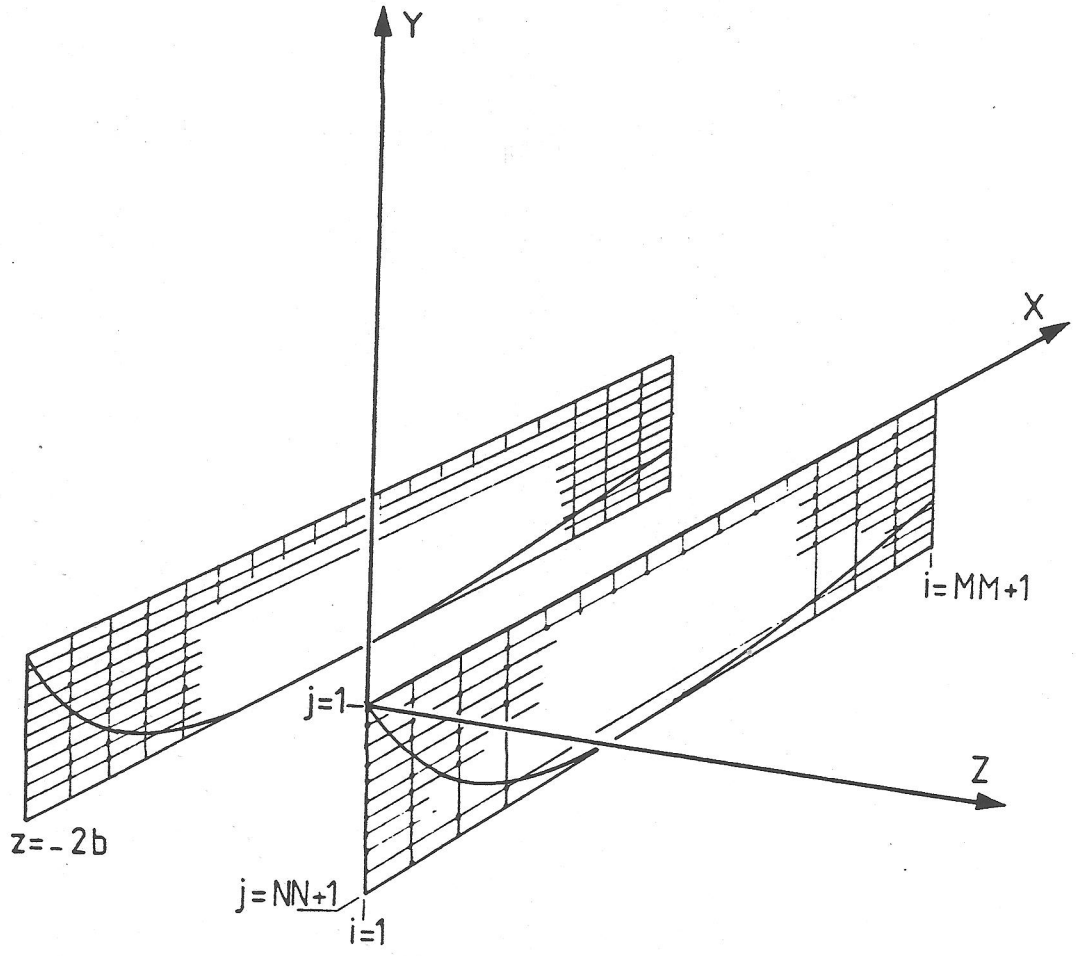

Figure 8: coordinate system used in the program CATREE

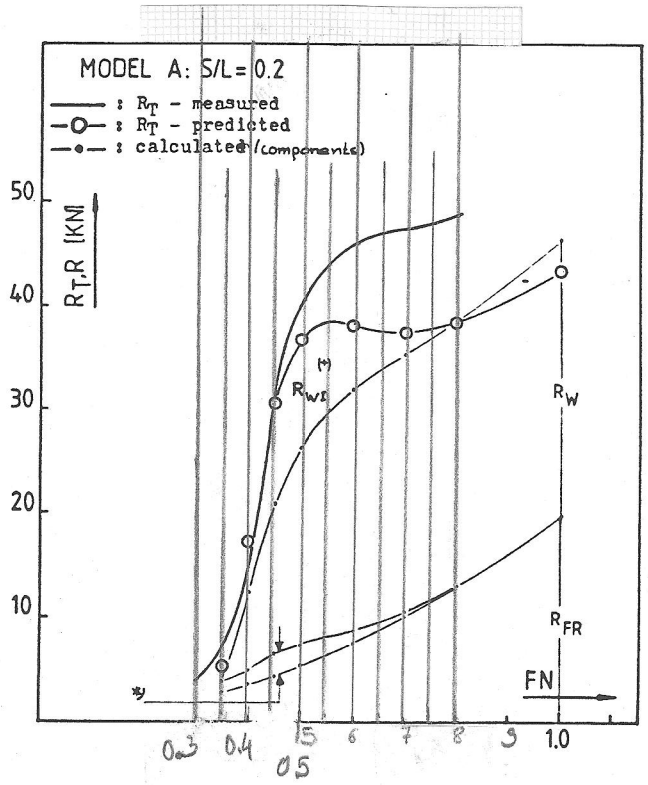

Figure 9: Results for model A ($S/L_{WL} = 0.2$)

*) note: indication to the formeffect in R_{FR}

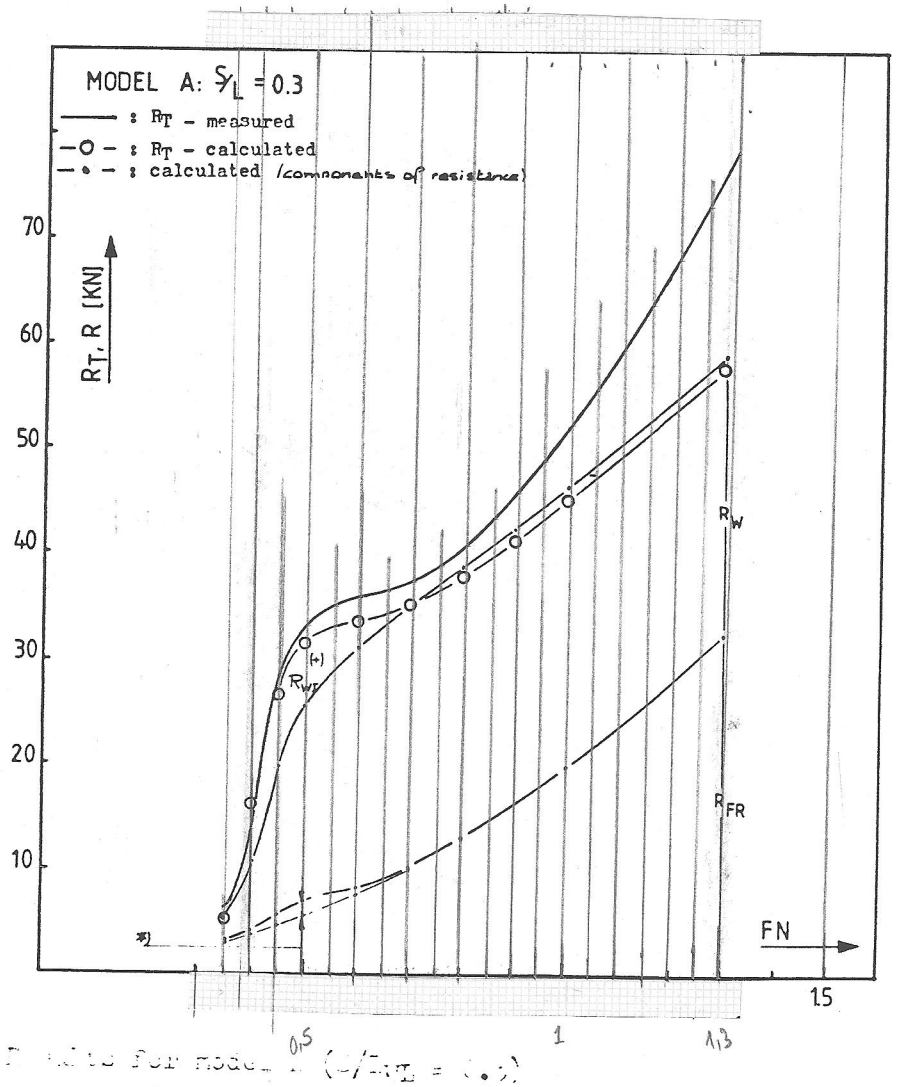

Fig. - Results for model A ($S/L_{WL} = 0.3$)

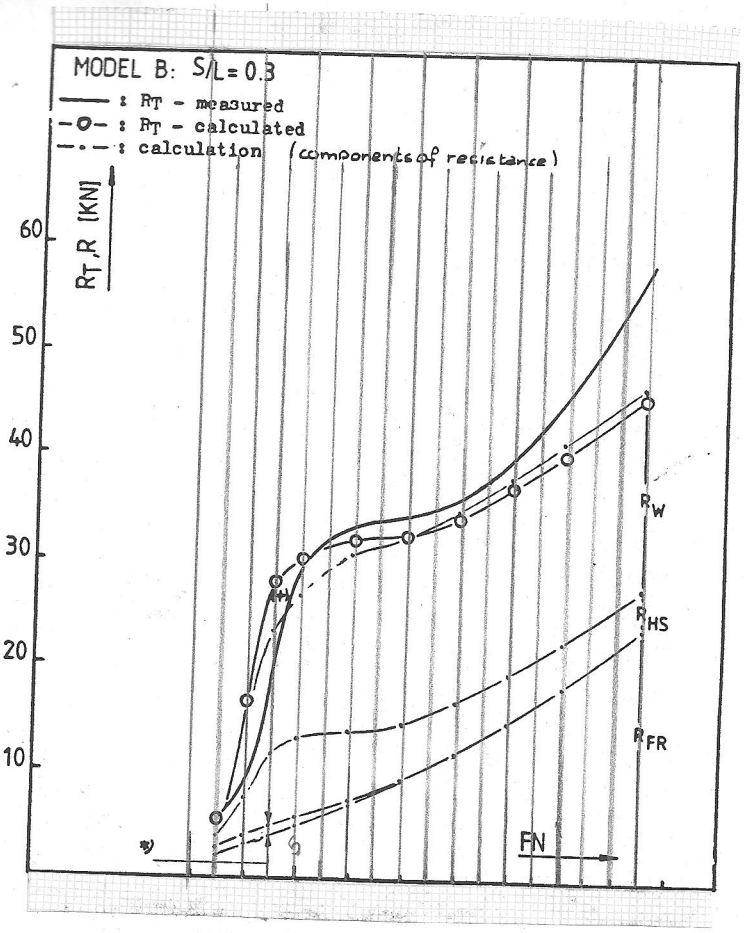

Figure 11: Results for model B: $S/L_{.I}$ = 0.3

*) = formeffect in R_{FR}

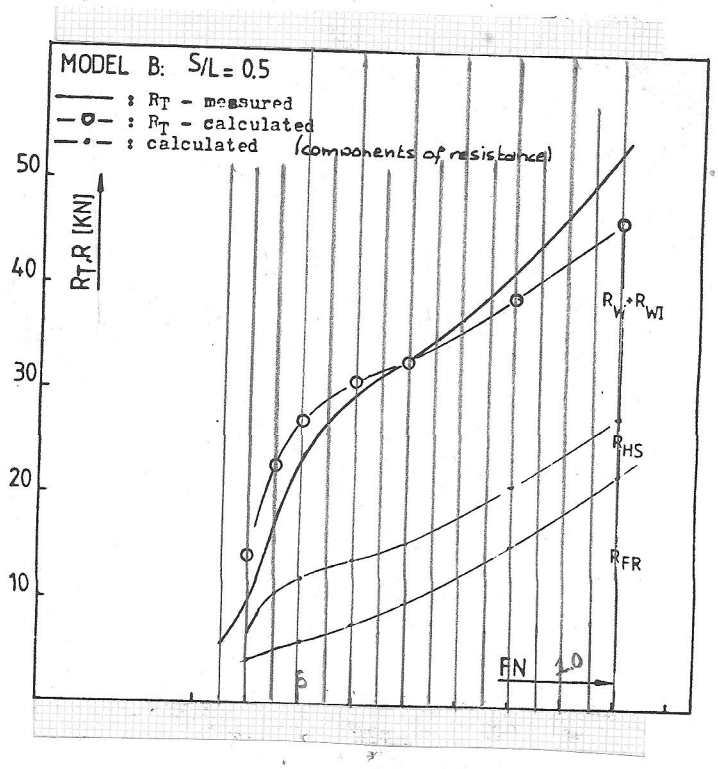

Figure 12: Results for model B: $S/L_{...}$ = 0.5

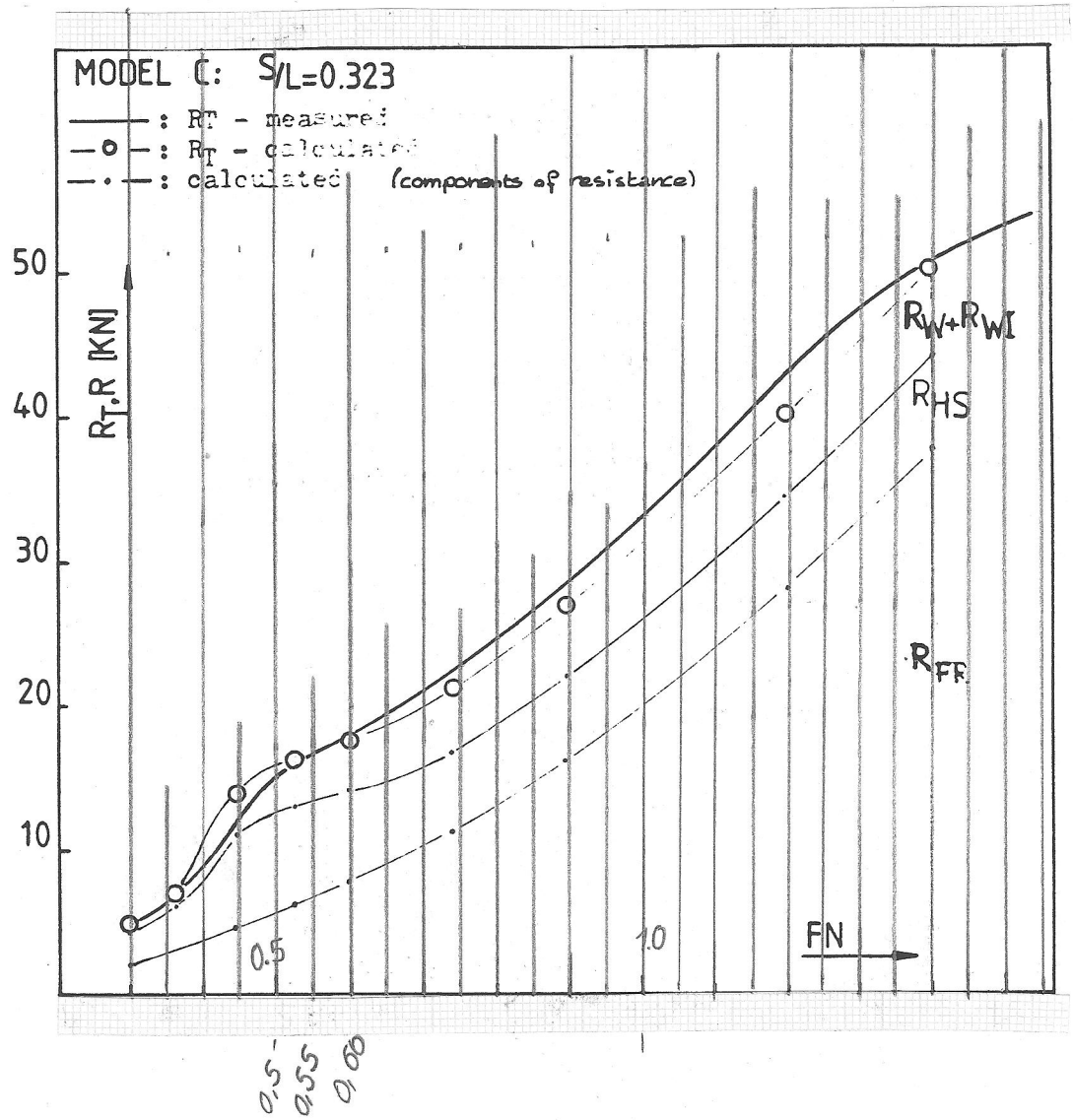

Figure 13: Results for model C

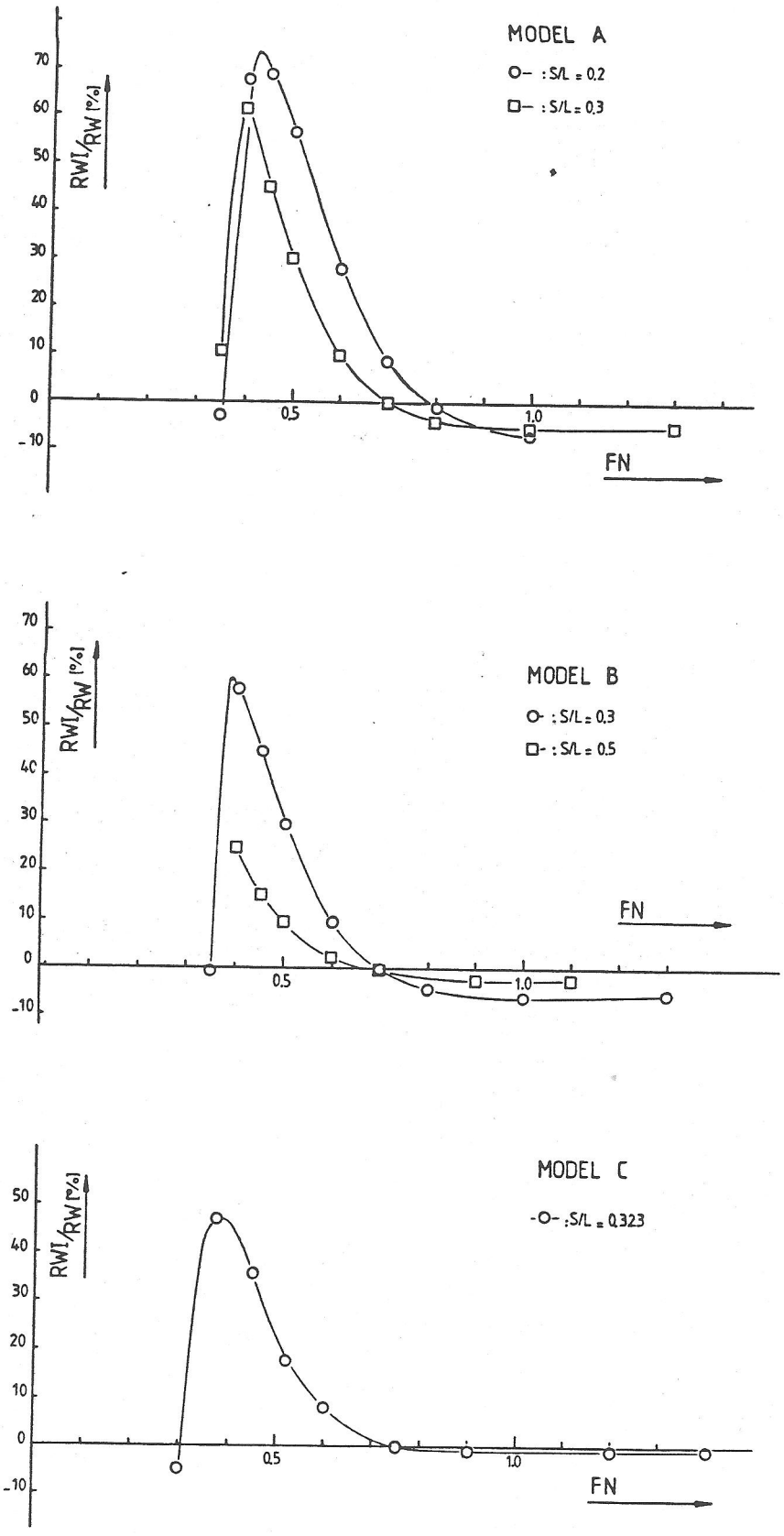

Figure 14: Calculated wave interference factors

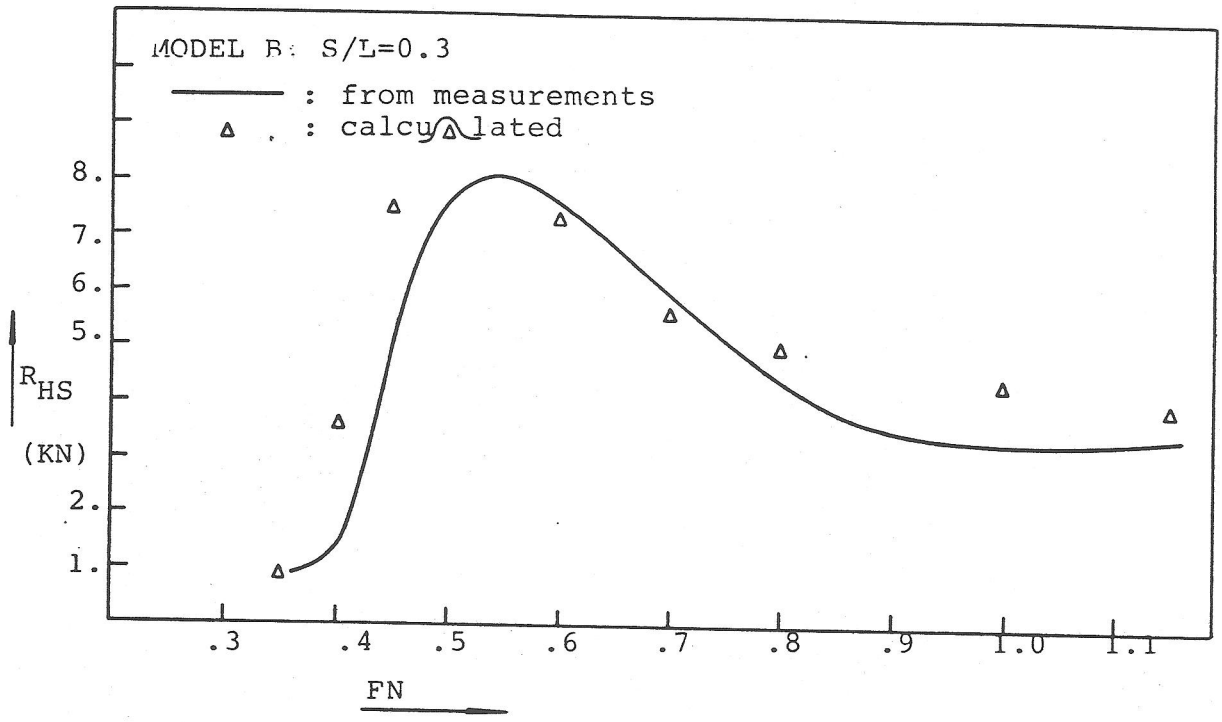

Figure 15: measured and calculated values of the hydrostatic component of the resistance

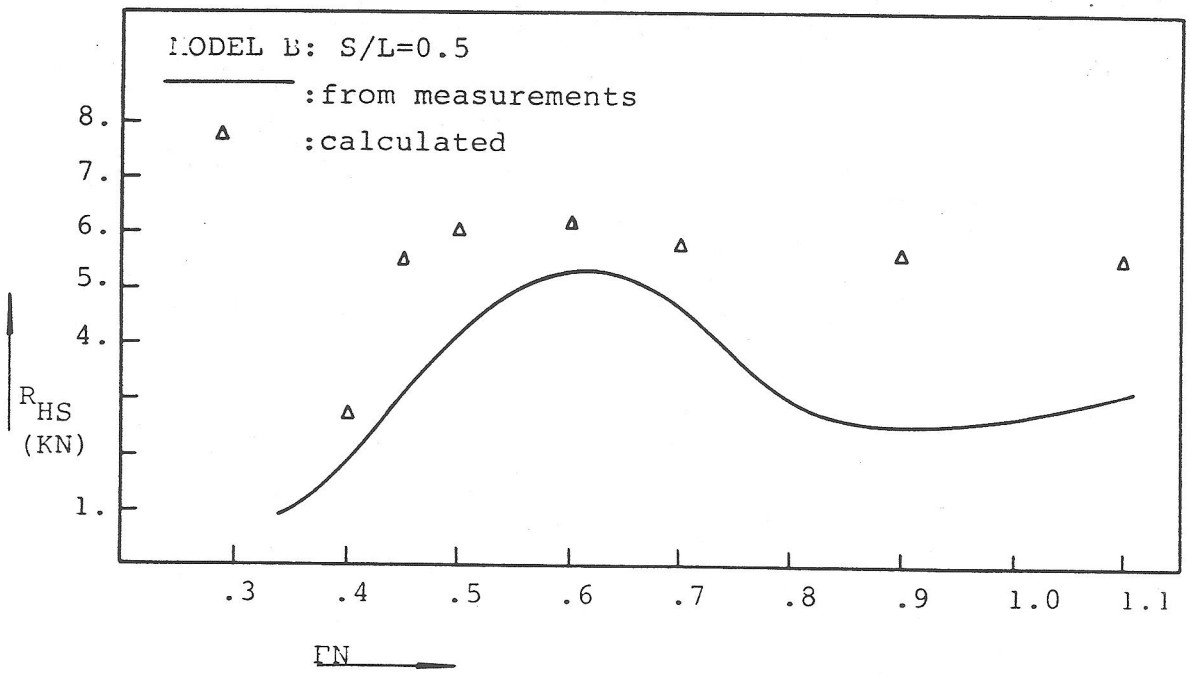

Figure 16: measured and calculated values of the hydrostatic component of the resistance

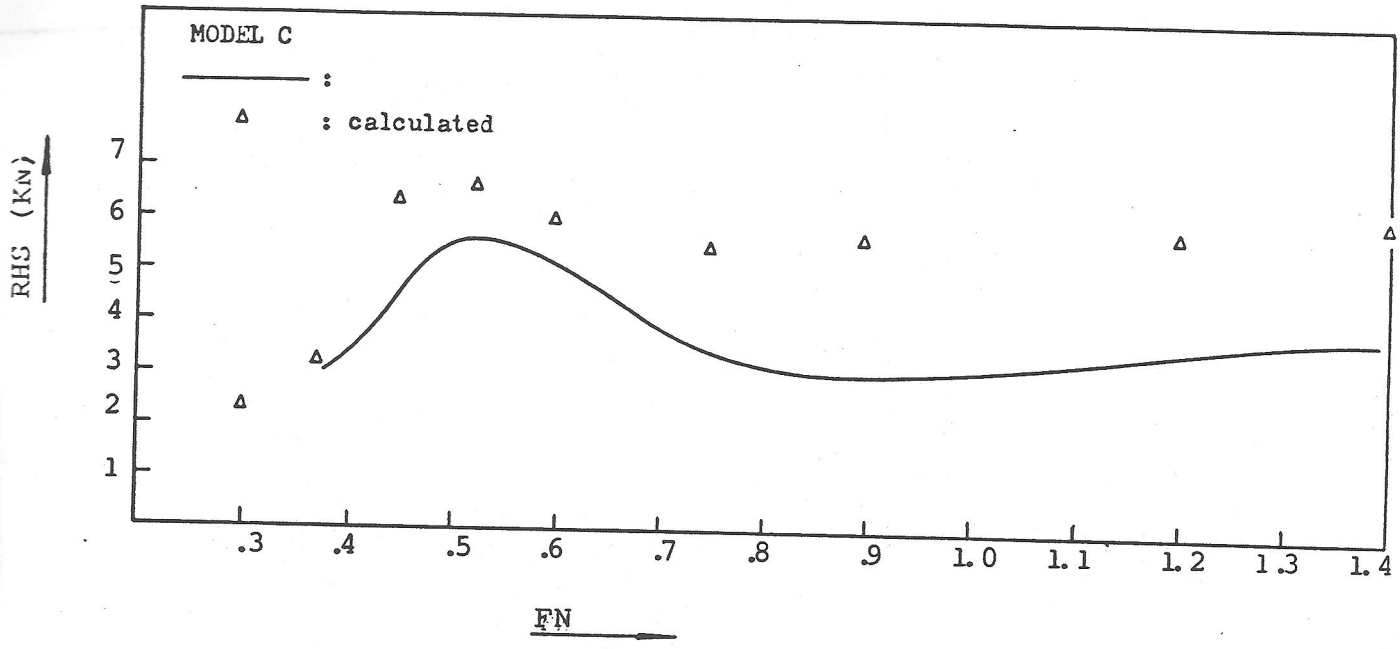

Figure 17: measured and calculated values of the hydrostatic component of the resistance

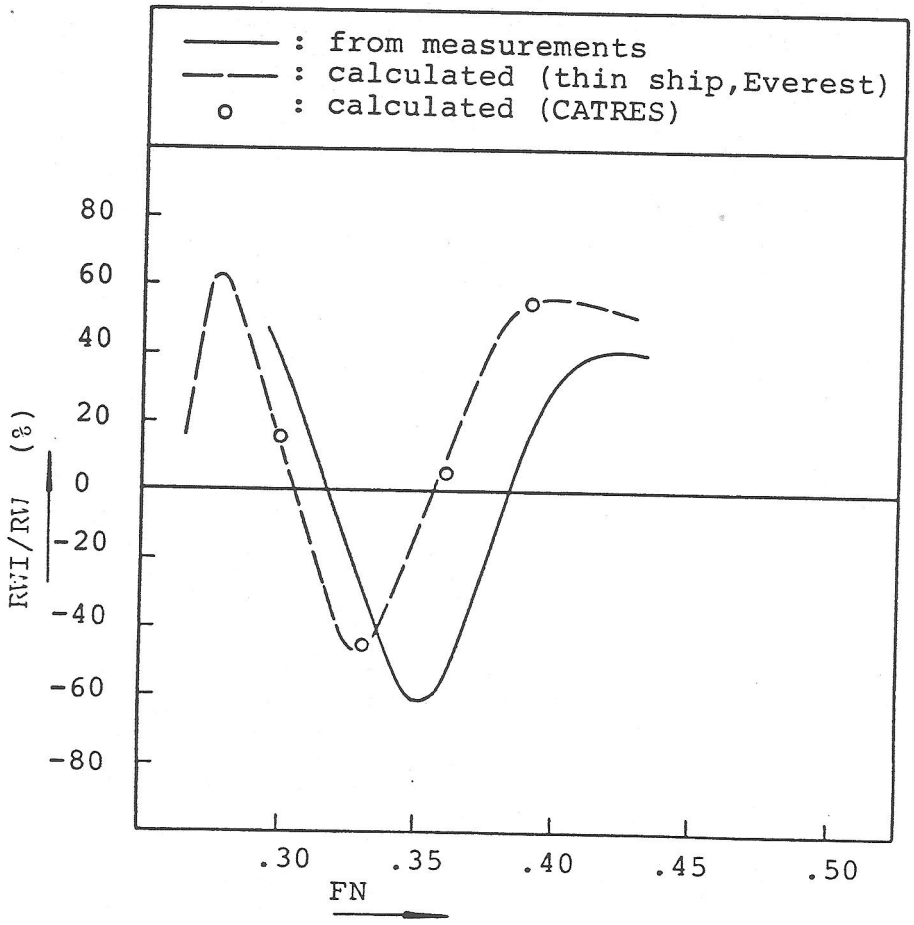

Figure 18: ratio of waveinterference- and waveresistance as function of the froudenumber (mathematical hullform)

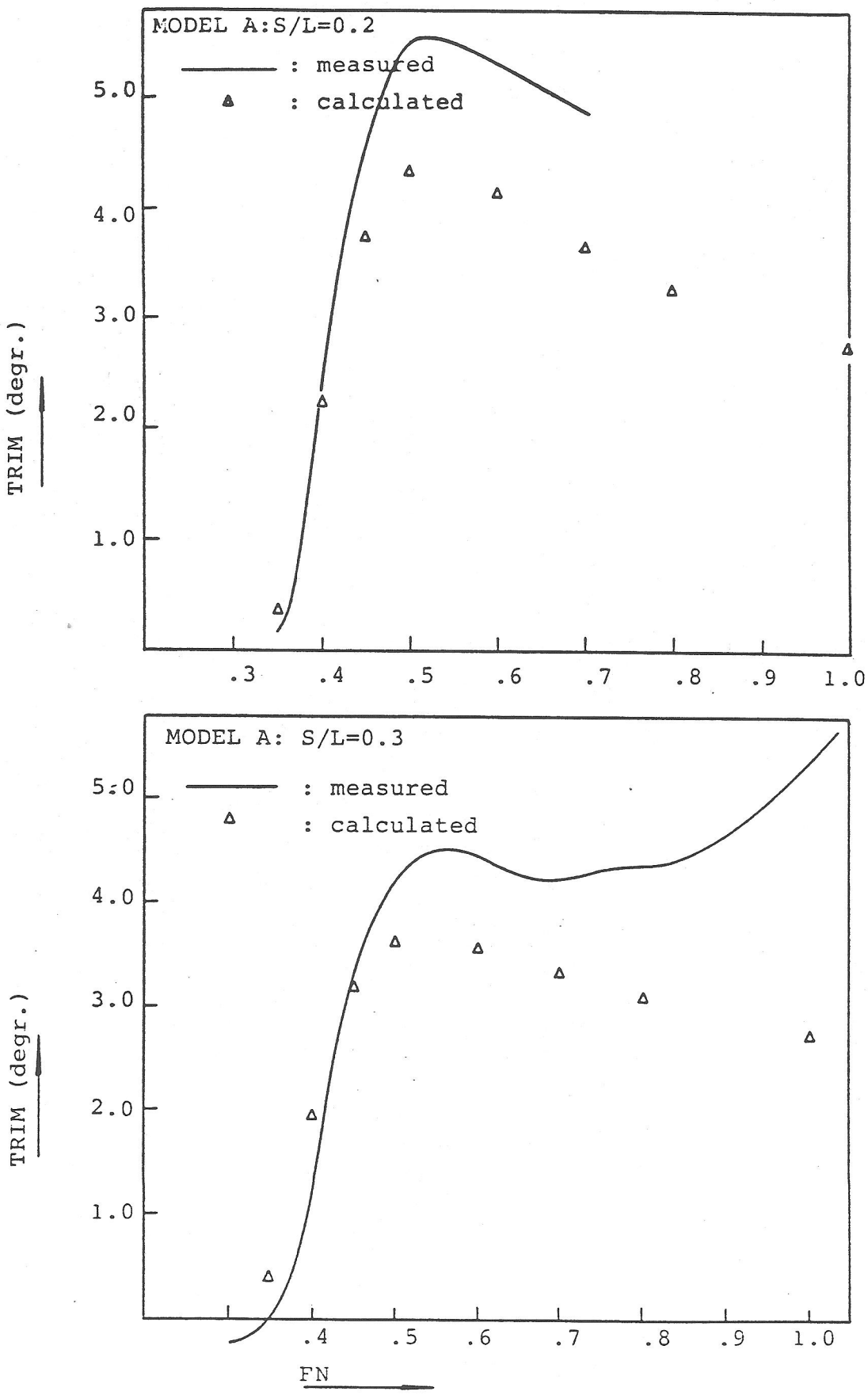

Figure 19: calculated and measured trim for model A

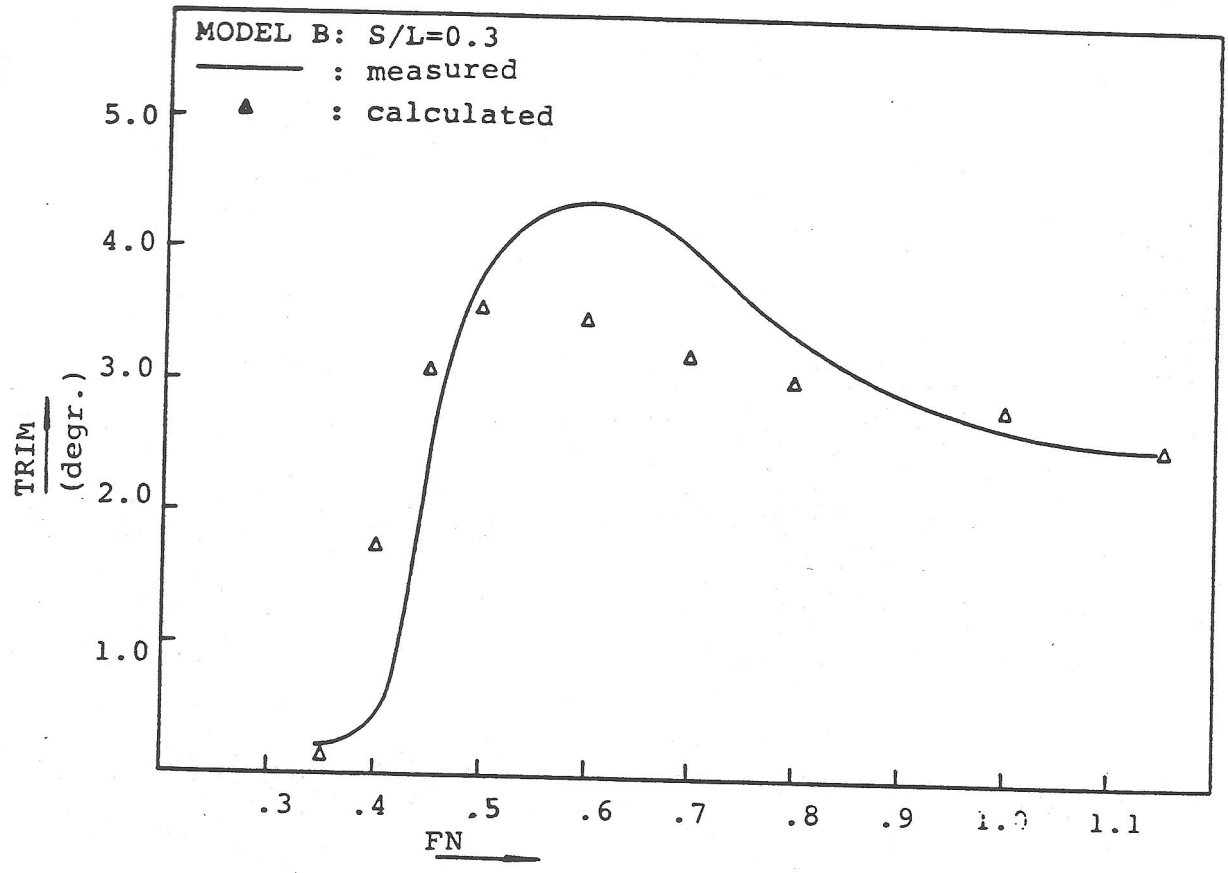

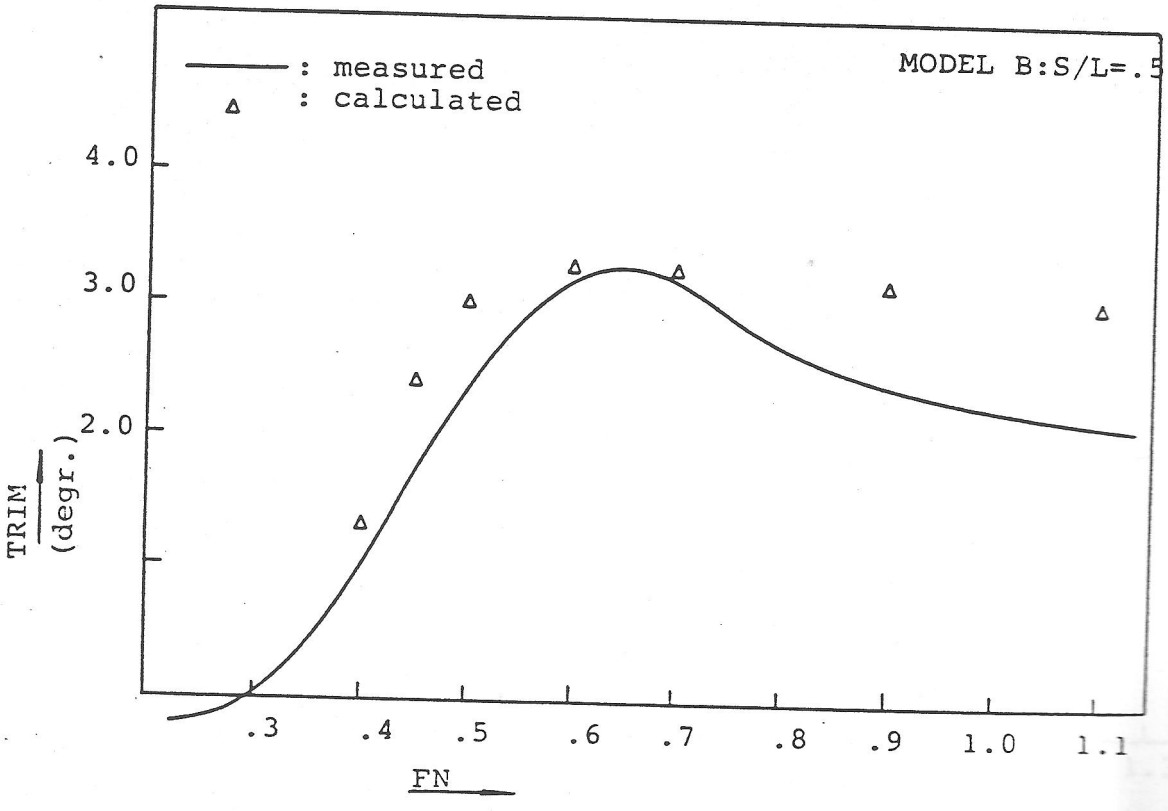

Figure 20: calculated and measured trim for model B

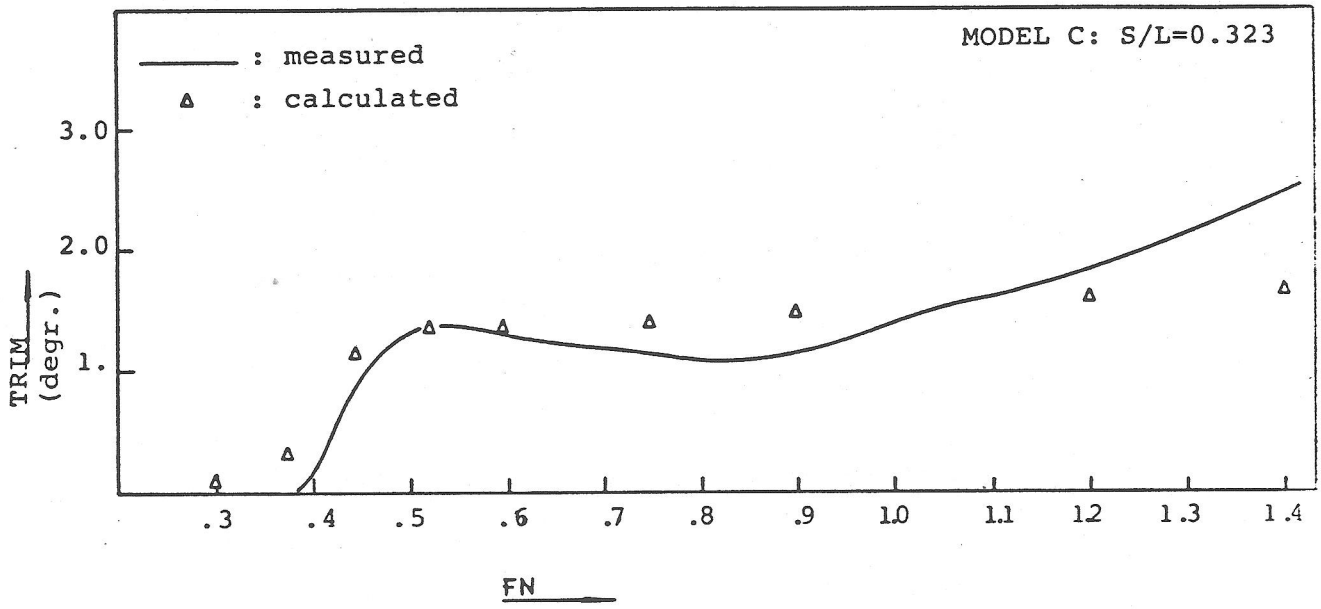

Figure 21: calculated and measured trim for model C

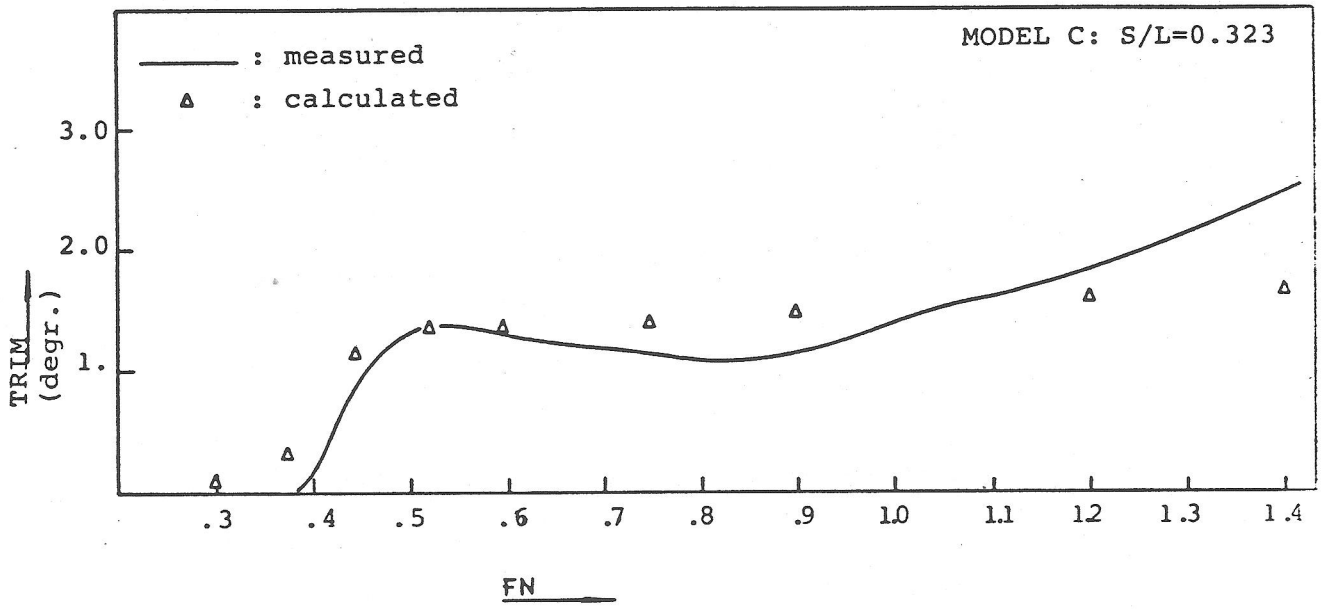

Figure 21: calculated and measured trim for model C

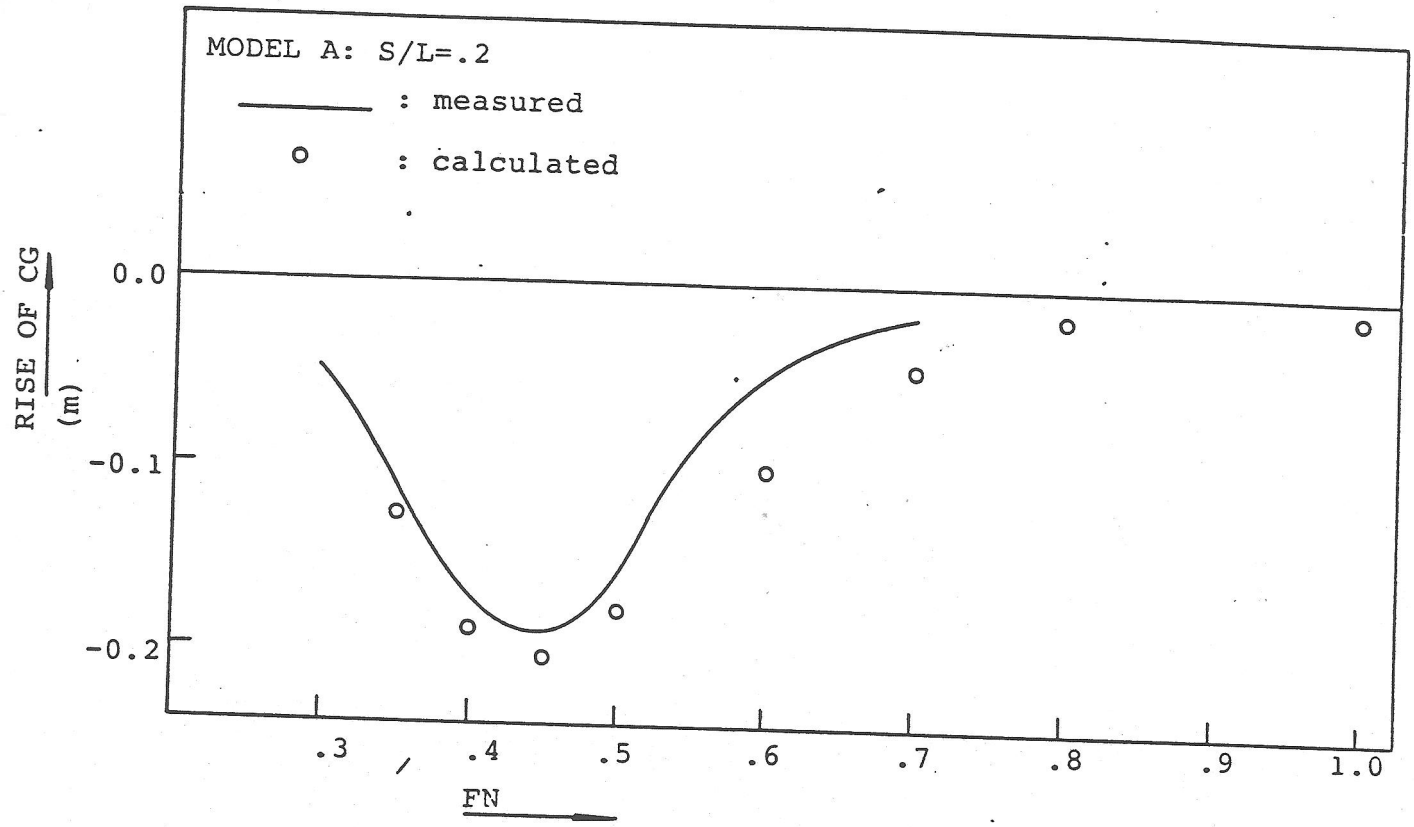

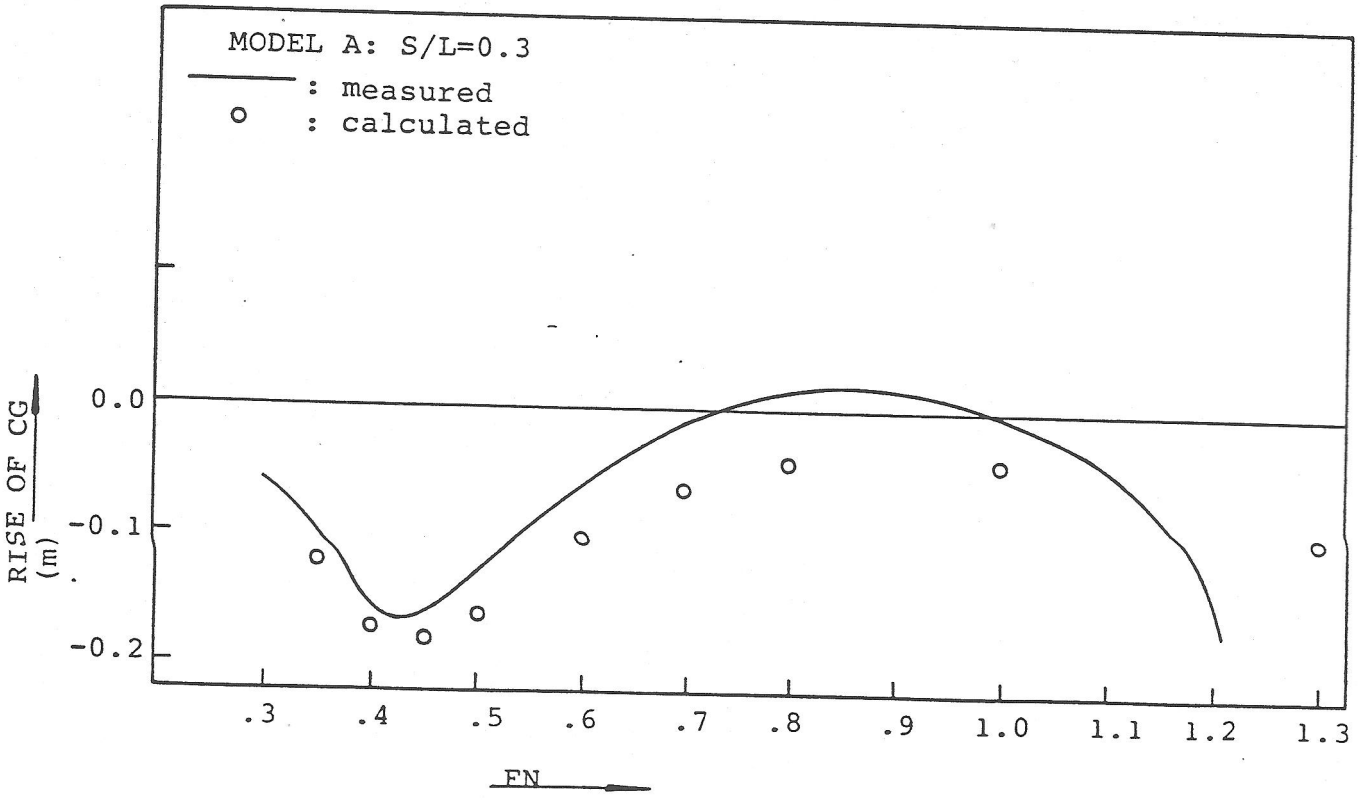

Figure 32: calculated and measured values of the rise of the centre of gravity, model A

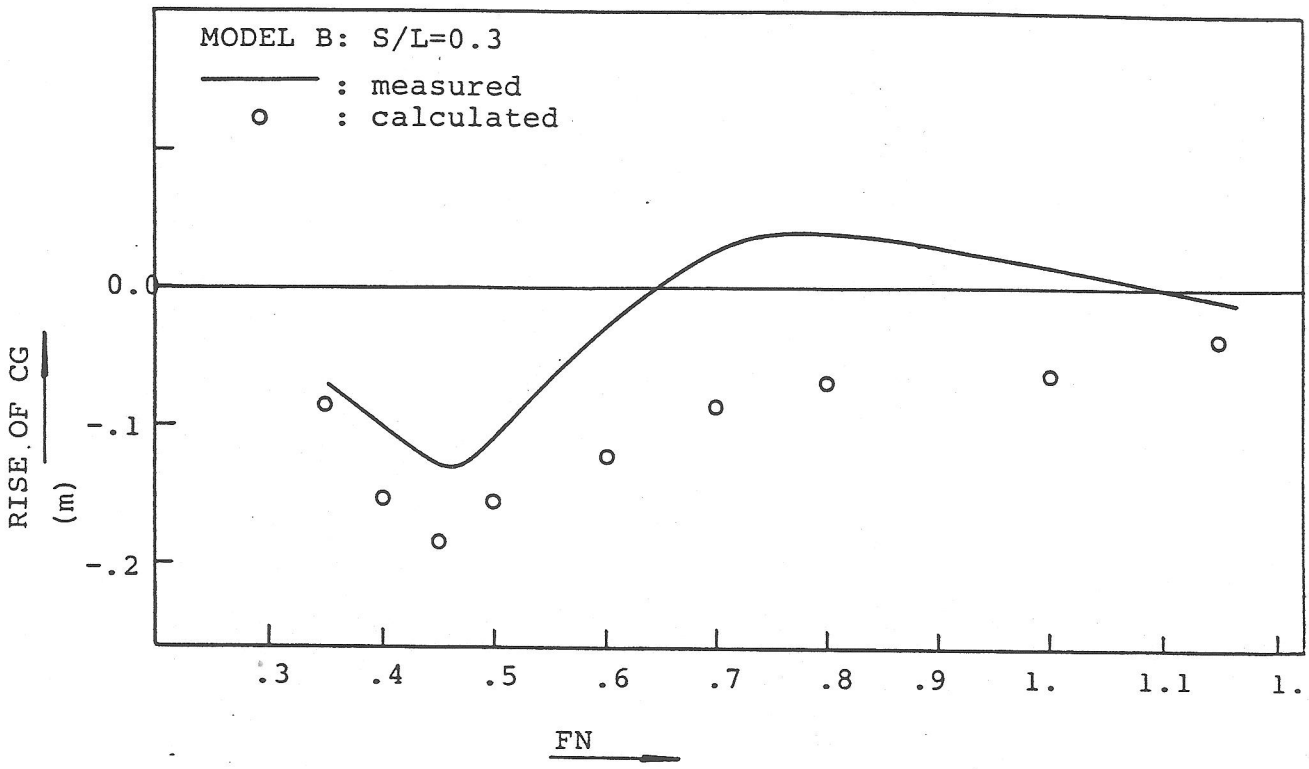

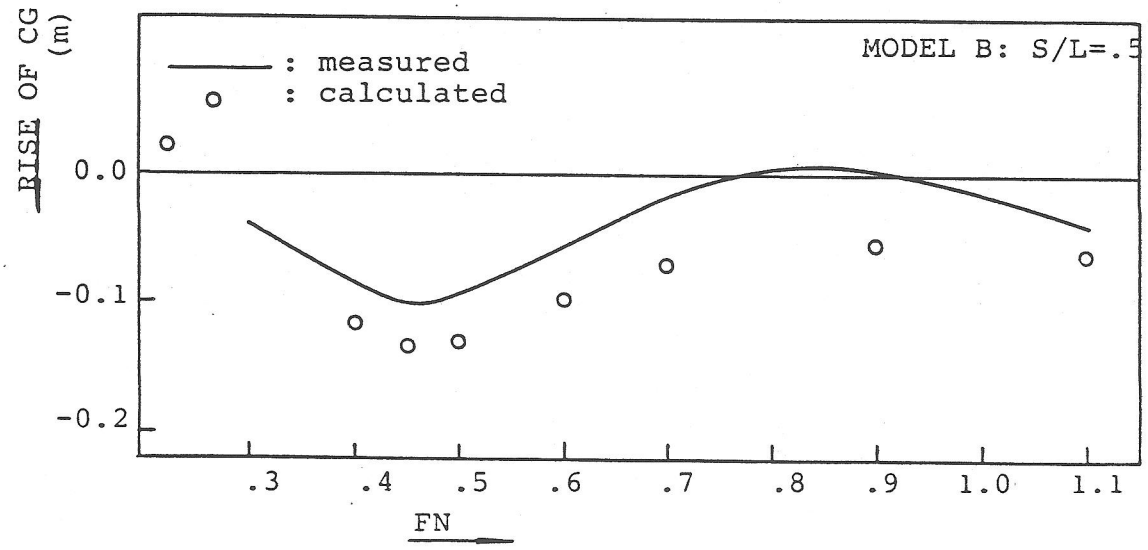

Figure 23: calculated and measured values of the rise of the centre of gravity, model B

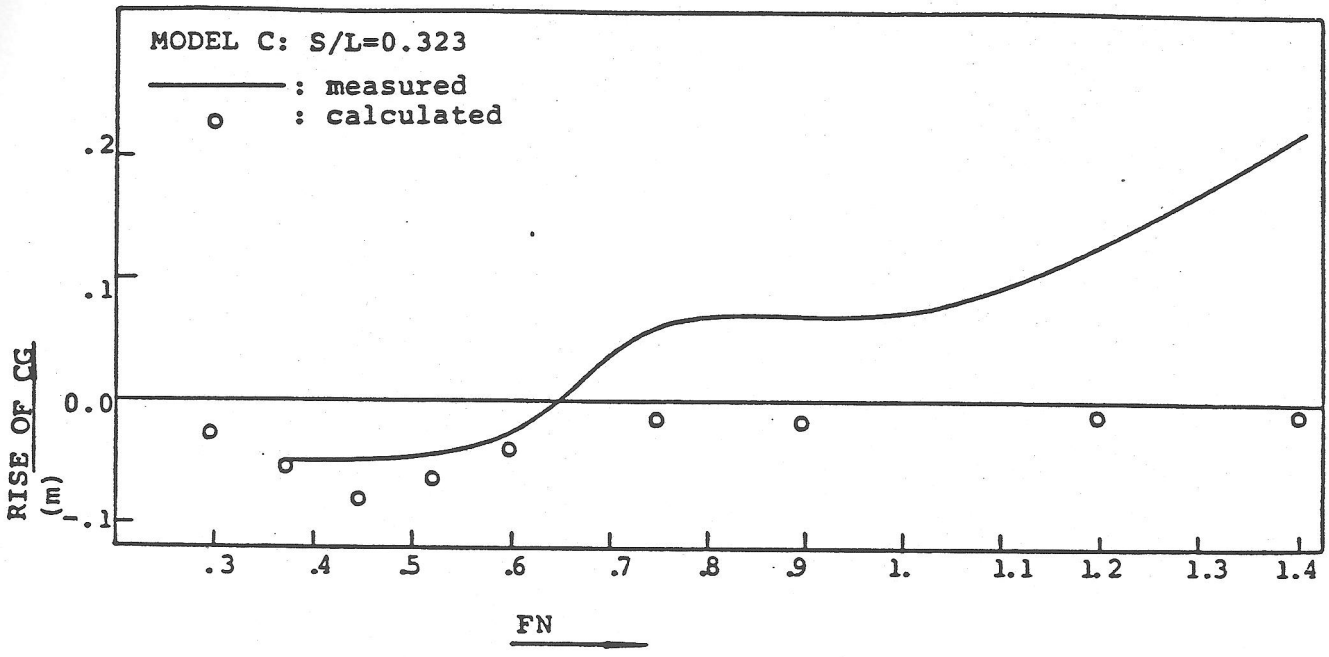

Figure 24: calculated and measured values of the rise of the centre of gravity, model C